Open access • Journal Article • DOI:10.1089/TEN.TEA.2009.0629

Human embryonic mesodermal progenitors highly resemble human mesenchymal stem cells and display high potential for tissue engineering applications.

Giuseppe Maria de Peppo, Sara Svensson, Maria Lennerås, Jane Synnergren ...+6 more authors

Institutions: University of Gothenburg, University of Skövde, Sahlgrenska University Hospital

Published on: 10 Mar 2010 - Tissue Engineering Part A (Mary Ann Liebert, Inc. 140 Huguenot Street, 3rd Floor New Rochelle, NY 10801 USA)

Topics: Adult stem cell, Stem cell, Clinical uses of mesenchymal stem cells, Stem cell transplantation for articular cartilage repair and Progenitor cell

TISSUE ENGINEERING: Part A
Volume 16, Number 7, 2010

DOI: 10.1089/ten.tea.2009.0629

Original Articles

Human Embryonic Mesodermal Progenitors Highly Resemble Human Mesenchymal Stem Cells and Display High Potential for Tissue Engineering Applications

Giuseppe Maria de Peppo, M.Sc.,[1,2] Sara Svensson, M.Sc.,[1,2] Maria Lennerås, M.Sc.,[2,3] Jane Synnergren, Ph.D.,[4,5] Johan Stenberg, M.Sc.,[5] Raimund Strehl, Ph.D.,[2,6] Johan Hyllner, Ph.D.,[2,6] Peter Thomsen, Ph.D.,[1,2] and Camilla Karlsson, Ph.D.[1,2]

Adult stem cells, such as human mesenchymal stem cells (hMSCs), show limited proliferative capacity and, after long-term culture, lose their differentiation capacity and are therefore not an optimal cell source for tissue engineering. Human embryonic stem cells (hESCs) constitute an important new resource in this field, but one major drawback is the risk of tumor formation in the recipients. One alternative is to use progenitor cells derived from hESCs that are more lineage restricted but do not form teratomas. We have recently derived a cell line from hESCs denoted hESC-derived mesodermal progenitors (hES-MPs), and here, using genome-wide microarray analysis, we report that the process of hES-MPs derivation results in a significantly altered expression of hESC characteristic genes to an expression level highly similar to that of hMSCs. However, hES-MPs displayed a significantly higher proliferative capacity and longer telomeres. The hES-MPs also displayed lower expression of HLA class II proteins before and after interferon-γ treatment, indicating that these cells may somewhat be immunoprivileged and potentially used for HLA-incompatible transplantation. The hES-MPs are thus an appealing alternative to hMSCs in tissue engineering applications and stem-cell-based therapies for mesodermal tissues.

Introduction

Tissue engineering is an emerging field of research aimed at regenerating functional tissues by combining cells with a supporting substrate. Stem cells are suitable cell types for this application owing to their expansion potential and ability to differentiate into a variety of tissues. Several different embryonic stem cell lines and adult stem cell sources have been used for this purpose,[1–4] underlining that some specific cell types may give better results in some particular applications. Among them, human embryonic stem cells (hESCs) constitute an important new resource in tissue engineering, mainly because of an extensive differentiation capacity and high proliferative potential. In fact, many adult organ-specific cells and stem cells show a limited proliferative capacity and, after long-term *in vitro* culture, lose their functional quality.[5] On the other hand, a major disadvantage with hESCs is the risk of tumor formation in the recipients.[6] hESC-derived mesodermal progenitors (hES-MPs) are derived from hESCs but are more lineage restricted and do not form teratomas *in vivo*. Similarly to hESCs, hES-MPs have a capacity for self-renewal and differentiation, but these properties are more limited.[7]

The derivation of hES-MPs from hESCs using different protocols has been described earlier.[8–12] None of these protocols address the important aspects of xeno-free derivation, robustness, and safety for the use in tissue engineering and cell therapies. We therefore recently developed an optimized protocol resulting in simple and reproducible derivation of hES-MPs from undifferentiated hESCs.[7] Multiple hES-MP cell lines have been derived and characterized using this protocol, including a xeno-free hES-MP cell line from xeno-free parental hESCs, and their differentiation capacity toward tissues of the mesodermal lineage, including the osteogenic, chondrogenic, and adipogenic lineages has been demonstrated.[7] The mesodermal commitment of the hES-MPs suggests that these cells are closely related to stem cells of the mesenchymal lineage and raises the urge for further

[1]Department of Biomaterials, Sahlgrenska Academy at University of Gothenburg, Göteborg, Sweden.
[2]BIOMATCELL VINN Excellence Center of Biomaterials and Cell Therapy, Göteborg, Sweden.
[3]TATAA Biocenter AB, Göteborg, Sweden.
[4]School of Life Sciences, University of Skövde, Skövde, Sweden.
[5]Department of Clinical Chemistry and Transfusion Medicine, Institute of Biomedicine, Sahlgrenska University Hospital, University of Gothenburg, Göteborg, Sweden.
[6]Cellartis AB, Göteborg, Sweden.

characterization. Human mesenchymal stem cells (hMSCs) represent a source of pluripotent cells that are already in various phases of clinical application. However, the use of hMSCs in tissue engineering has been hampered largely due to their low proliferation, finite life span, and gradual loss of their stem cell properties during *ex vivo* expansion.[5]

Today, the transcriptional changes occurring during hES-MP derivation have not been studied and it is not either known how closely the hES-MPs resemble hMSCs. There is further a lack of knowledge concerning the immunological properties of these hES-MPs as well as their regulation of senescence and proliferative capacity. These questions are a prerequisite to investigate in order to replace hMSCs with hESC-derived progenitor cells in future tissue engineering applications, which prompted us to comprehensively study these issues.

Materials and Methods

Cell types and culture conditions

The undifferentiated hESC lines used in this study were the SA167, SA002.5, and SA461, derived and characterized at Cellartis AB, Gothenburg, Sweden. Detailed protocols are available at Cellartis (www.cellartis.com). The hES-MP cell lines were derived from the three undifferentiated hESC lines described above, as previously reported.[7] hMSCs were isolated from bone marrow aspirates from the iliac crest of patients undergoing spinal fusion (age range 13–20 years) and expanded as described previously.[13] The cells were harvested for RNA isolation in passage 3 when the cells reached 80% confluence. The donation of bone marrow was approved by the ethics committee at the Medical Faculty at Gothenburg University (Dnr. 532-04).

Flow cytometry analysis

Flow cytometry analysis was used to confirm isolation and enrichment of hMSCs, verify microarray results, and examine expression of immunological markers. To verify enrichment of hMSCs, cells were stained with CD34-PerCP, CD45-FITC, CD105-FITC, and CD166-PE (all from Ancell). To verify the microarray results, hMSCs, hES-MPs, and hESCs were stained with CD44-FITC (BD Biosciences), CD58-PE (BD Biosciences), CD47-FITC (BD Biosciences), and CD166-PE. Expression of immunological markers was studied in both hMSCs and hES-MPs at low and high passage (defined as 5 and 50 population doublings [PDs], respectively) as well as before and after a 5-day treatment with interferon-γ (IFN-γ) (100 U/mL; R&D Systems Europe). The cells were then stained with HLA-ABC-FITC, HLA-DR-FITC, CD80-FITC (all from BD Biosciences), and CD86-PerCP-Cy5 (Ancell). All samples were analyzed using the FACS Aria flow cytometer (Becton Dickinson) using FACS Diva software (Becton Dickinson).

RNA isolation

Total RNA was extracted using the RNeasy® Minikit (Qiagen GmbH) according to manufacturer's instructions. DNAse treatment was performed to eliminate any contamination from genomic DNA according to Qiagen RNase Free DNase Set (Qiagen GmbH) protocol.

Microarray analysis

RNA from hESCs, hES-MPs, and hMSCs was subjected to gene expression analysis using the oligonucleotide microarray HG-U133plus2.0 (Affymetrix) according to manufacturer's recommendations. Raw expression data were normalized and subsequently analyzed with GeneChip Operating Software 1.4 (GCOS; Affymetrix). Comparative and statistical analyses were performed with the BIORETIS Web tool (www.bioretis-analysis.de). Genes were selected for further analysis only if (1) the absolute call for the gene was present for at least one of the three cell types, (2) three out of three comparisons had to be considered increased or decreased according to Affymetrix algorithm, and (3) the average fold change (FC) should be at least twofold. Using these qualitative and quantitative filtering criteria, we performed two comparative analyses, one between hES-MPs and hESCs and the other between hES-MPs and hMSCs. Functional classification into five different categories—transcription factors, extracellular matrix components, growth factors, membrane receptors, and cell adhesion molecules—was performed using annotations from the Gene Ontology Annotation Database.[14] Further, expression of 48 genes known to be overexpressed in hESCs compared with differentiated cell types, 40 genes specifically expressed in hESCs, and 30 selected genes underexpressed in hESCs compared with differentiated cell types was investigated.[15] For these genes, the mean expression level from different probe sets of each gene was calculated and reported in Table 1A–C. The significance level was determined applying the Welch's *t*-test on log2-transformed signal values. Hierarchical cluster analysis was performed using log2-transformed signals of all the replicates using Genesis 1.7.3 software.[16]

To explore the similarity in global gene expression pattern across investigated samples, the correlation was calculated using standard function in R statistical software. Spearman was used as correlation coefficient, and genes with missing values were excluded from the calculation. The interpretation of this analysis is as follows: 1 means perfect correlation, −1 means negative correlation, and 0 means no correlation.

The percentage of genes with an FC ≤ 3 between pairs of samples was calculated for all three comparisons (hES-MPs vs. hMSCs, hES-MPs vs. hESCs, and hMSCs vs. hESCs). This FC-threshold was defined based on the results from comparisons of the biological replicates. To define the background variation, the FCs between pair-wise replicates were calculated, and the results showed that 90% of all the genes have an FC ≤ 3 between any two replicates of a sample.

To observe the similarity in global gene expression across the investigated cell samples, scatter plots were generated between average signals of pairs of samples using standard function in R.

Analysis of protein interaction networks

To investigate possible interactions among proteins from differentially expressed genes (defined by having an FC of at least 10) between hES-MPs and hESCs or hES-MPs and hMSCs and to identify hub proteins, the search tool STRING (http://string.embl.de) was used to mine for recurring instances of neighboring genes. A gene of interest was classified as a hub if it had at least five interactions with other genes.[14]

Table 1A. Microarray Results of 40 Genes Specifically Expressed in Human Embryonic Stem Cells

Gene name	*Gene abbreviation*	*FC hES-MP vs. hESCs*	p	*FC hES-MP vs. hMSCs*	p
Abhydrolase domain containing 9	*ABHD9*	**–17.4**	0.0000	1.5	0.3031
Barren homolog protein 1	*BRRN1*	−4.2	0.0087	**22.6**	0.0000
Chromosome 14 open reading frame 115	*C14orf115*	**–14.3**	0.0000	1.7	0.1378
Cell division cycle 25 homolog A	*CDC25A*	**–10.7**	0.0000	6.1	0.2463
CHK2 checkpoint homolog	*CHEK2*	**–4.2**	0.0000	−1.1	0.6316
Claudin 6	*CLDN6*	**–213.7**	0.0000	0.6	0.2859
Chromosome X open reading frame 15	*CXorf15*	**–3.2**	0.0000	1.1	0.5589
Cytochrome P450, family 26, subfamily A1	*CYP26A1*	**–81.9**	0.0000	2.1	0.2116
Defective in sister chromatid cohesion protein 1	*DCC1*	**–3.8**	0.0081	1.3	0.3638
DNA (cytosine-5-)-methyltransferase 3 alpha	*DNMT3A*	**–4.3**	0.0021	0.7	0.2329
Deoxythymidylate kinase	*DTYMK*	1.1	0.4926	1.4	0.4324
EPH receptor A1	*EPHA1*	**–21.3**	0.0002	0.0	0.4250
Ets variant gene 4	*ETV4*	**–3.5**	0.0001	2.1	0.0209
LINE-1 type transposase domain containing 1	*FLJ10884*	**–226.3**	0.0000	0.3	0.4757
FLJ20105 protein	*FLJ20105*	−1.7	0.0047	**17.7**	0.0000
Apoptosis enhancing nuclease	*FLJ12484*	−1.7	0.0070	1.3	0.1510
Growth differentiation factor 3	*GDF3*	**–9.3**	0.0000	1.1	0.5610
Gap junction protein, gamma 1	*GJA7*	0.6	0.4198	**6.9**	0.0033
G protein-coupled receptor 19	*GPR19*	**–24.6**	0.0000	2.3	0.0391
G protein-coupled receptor 23	*GPR23*	**–4.3**	0.0012	2.1	0.0069
Helicase	*HELLS*	−2.5	0.0933	**19.5**	0.0011
HESX homeobox 1	*HESX1*	**–84.4**	0.0000	**–4.8**	0.0007
KIAA0523 protein	*KIAA0523*	−2.7	0.0356	−3.4	0.0614
Lin-28 homolog	*LIN28*	**–496.5**	0.0000	2.7	0.0001
Minichromosome maintenance complex 10	*MCM10*	**–4.3**	0.0000	**9.7**	0.0097
Dysbindin	*MGC3101*	−2.3	0.0782	2.6	0.2980
V-myb myeloblastosis viral oncogene-like 2	*MYBL2*	**–8.5**	0.0000	3.0	0.0000
Nanog homeobox	*NANOG*	**–1482.0**	0.0000	**–4.3**	0.0001
Origin recognition complex, subunit 1-like	*ORC1L*	**–16.1**	0.0000	**4.6**	0.5496
Origin recognition complex, subunit 2-like	*ORC2L*	−2.6	0.0000	1.1	1.0000
POU class 5 homeobox 1	*POU5F1*	**–445.7**	0.0000	1.0	0.0558
PR domain containing 14	*PRDM14*	**–10.1**	0.0000	2.2	0.0007
Chromosome 2 open reading frame 56	*PRO1853*	−2.2	0.0045	0.5	0.2072
PWP2 periodic tryptophan protein homolog	*PWP2H*	−0.8	0.0915	1.2	0.4675
RNA binding motif protein 14	*RBM14*	**–7.7**	0.0000	2.4	0.0000
RNA, U3 small nucleolar interacting protein 2	*RNU3IP2*	−1.8	0.0127	1.5	0.0032
Solute carrier family 5 member 6	*SLC5A6*	**–5.4**	0.0000	1.7	0.0012
SLD5 homolog	*SLD5*	−2.5	0.0337	4.0	0.2560
Teratocarcinoma-derived growth factor 1	*TDGF1*	**–315.2**	0.0000	1.5	0.0145
Zic family member 3	*ZIC3*	**–51.6**	0.0000	−1.1	0.9404

Genes significantly regulated are in boldface.
FC, fold change; hESC, human embryonic stem cell; hES-MP, hESC-derived mesodermal progenitor; hMSC, human mesenchymal stem cell.

Quantitative real time-polymerase chain reaction

Microarray results were verified using real-time polymerase chain reaction (PCR), flow cytometry, and immunohistochemistry. For real-time PCR, reverse transcription was carried out using iScript cDNA Synthesis Kit (Bio-Rad) according to manufacturer's instructions. Design of primers for *TDGF*, *TGF-β2R*, *RUNX2*, *COL1A1*, *LHX8*, and *BMP2R* was performed using the Primer3 Web-based software. Primer sequences and detailed protocols are available at TATAA Biocenter AB, Göteborg, Sweden (www.tataa.com). Statistical analysis for real-time PCR data was performed using the Mann–Whitney test. Differences were accepted to be statistically significant at $p \leq 0.05$ (*).

Immunohistochemistry

Monoclonal antibodies against the pluripotency markers OCT4 and NANOG were used to immunohistochemically verify the microarray results. The procedure used for the analysis has previously been described.[17]

Proliferative capacity

To compare the expansion ability of hMSCs and hES-MPs, cells were expanded as described above and passaged when one of them reached 80% confluence. At each passage, cells were counted in a hemocytometer and the number of cell doublings was calculated.

Telomerase activity

Telomerase activity was evaluated using the *TeloTAGGG* Telomerase PCR ELISA^{PLUS} kit (Roche Diagnostics Scandinavia AB). Both hMSCs and hES-MPs at low and high passage were analyzed according to manufacturer's recommendations. The PCR was performed using a Thermal Cycler 2720

Table 1B. Microarray Results of 48 Genes Known to Be Overexpressed in Human Embryonic Stem Cells Compared with Differentiated Cell Types

Gene name	*Gene abbreviation*	*FC hES-MP vs. hESCs*	p	*FC hES-MP vs. hMSCs*	p
Aminoadipate-semialdehyde synthase	*AASS*	**–5.3**	0.0000	−1.7	0.3257
Alkaline phosphatase, liver/bone/kidney	*ALPL*	**–27.3**	0.0000	−4.0	0.0546
Bone morphogenetic protein receptor, type 1A	*BMPR1A*	**–3.0**	0.0000	1.3	0.0003
BUB1 budding uninhibited by benzimidazoles 1	*BUB1*	**–6.0**	0.0212	4.0	0.2569
CCAAT/enhancer binding protein zeta	*CEBPZ*	**–3.7**	0.0000	1.1	0.1389
Collapsin response mediator protein 1	*CRMP1*	**–4.1**	0.0000	2.7	0.0000
Cytochrome P450, family 26, subfamily A 1	*CYP26A1*	**–81.9**	0.0000	2.1	0.2116
DNA (cytosine-5-)-methyltransferase 3 beta	*DNMT3B*	**–79.4**	0.0000	1.5	0.0003
Developmental pluripotency associated 4	*DPPA4*	**–21.0**	0.0000	7.9	0.1538
GABA A receptor, beta 3	*GABRB3*	**–34.4**	0.0004	−0.2	0.3643
Galanin prepropeptide	*GAL*	**–16.3**	0.0143	2.6	0.0543
Growth differentiation factor 3	*GDF3*	**–9.3**	0.0000	1.1	0.5610
Glypican 4	*GPC4*	**–58.2**	0.0000	**–6.1**	0.0017
Helicase	*HELLS*	−2.5	0.0933	**19.5**	0.0011
HRAS-like suppressor 3	*HRASLS3*	1.4	0.1165	−1.6	0.0071
Heat shock 70 kDa protein 4	*HSPA4*	**–3.5**	0.0000	1.6	0.0285
Indoleamine-pyrrole 2,3 dioxygenase	*IDO1*	**–5.5**	0.0021	1.1	0.5527
Integrin beta 1 binding protein 3	*ITGB1BP3*	**–38.2**	0.0000	−1.3	0.3081
KIAA0523 protein	*KIAA0523*	**–2.7**	0.0356	−3.4	0.0614
Leukocyte cell derived chemotaxin 1	*LECT1*	**–20.2**	0.0000	1.7	0.1637
Left-right determination factor 1	*LEFTY1*	**–14.3**	0.0014	−1.1	0.3309
Lin-28 homolog (C. elegans)	*LIN28*	**–496.5**	0.0000	2.7	0.0977
Mannose-6-phosphate receptor	*M6PR*	0.6	0.0056	1.8	0.0003
Minichromosome maintenance complex 5	*MCM5*	**–9.5**	0.0000	**9.2**	0.0002
Microsomal glutathione S-transferase 1	*MGST 1*	−1.3	0.1750	−1.2	0.2586
MutS homolog 2	*MSH2*	**–8.0**	0.0000	−1.0	1.0000
Methylenetetrahydrofolate dehydrogenase	*MTHFD1*	1.3	0.0270	0.1	0.5060
Nanog homeobox	*NANOG*	**–1482.0**	0.0000	**–4.3**	0.0000
Nuclear autoantigenic sperm protein	*NASP*	**–4.7**	0.0745	1.6	0.0307
Origin recognition complex, subunit 1-like	*ORCIL*	**–16.1**	0.0000	**4.6**	0.0001
PHD finger protein 17	*PHF17*	**–4.0**	0.0000	−2.0	0.0002
Pim-2 oncogene	*PIM2*	**–4.5**	0.0000	−1.0	0.9369
Phosplipase A2, group XVI	*PLA2G16*	**–35.1**	0.0000	**–17.1**	0.0000
POU class 5 homeobox 1	*POU5F1*	**–445.7**	0.0000	1.0	1.0000
Phosphoribosyl pyrophosphate amidotransferase	*PPAT*	−1.7	0.0368	0.5	0.5055
PC4 and SFRS1 interacting protein 1	*PSIP1*	**–3.7**	0.0384	−0.7	0.4442
Sema domain 6A	*SEMA6A*	**–37.3**	0.1394	1.9	0.3944
Selenophosphate synthetase 1	*SEPHS1*	**–7.5**	0.0000	2.0	0.0130
Solute carrier family 16, member 1	*SLC16A1*	**–3.8**	0.0000	1.7	0.0024
Small nuclear ribonucleoprotein polypeptide N	*SNRPN*	−2.1	0.2068	1.5	0.4131
SNRPN upstream reading frame	*SNRPN*	**–4.2**	0.0000	2.2	0.0037
SRY (sex determining region Y)-box 2	*SOX2*	**–22.5**	0.0001	3.6	0.3468
Teratocarcinoma-derived growth factor 1	*TDGF1*	**–315.2**	0.0000	1.5	0.4168
Telomeric repeat binding factor 1	*TERF1*	**–10.7**	0.0000	0.1	0.4638
UDP-glucose pyrophosphorylase 2	*UGP2*	−2.6	0.0010	−0.1	0.4705
Uracil-DNA glycosylase	*UNG*	**–3.4**	0.0000	1.4	0.0213
Ubiquitin specific peptidase 9, X-linked	*USP9X*	−2.0	0.1573	−0.3	0.0534
Zic family member 3	*ZIC3*	**–51.6**	0.0000	−1.1	0.9250

Genes significantly regulated are in boldface.

(Applied Biosystems), and the absorbance was read at 450 nm using the iEMS reader MF (Labsystems) microtiter plate reader and Ascent software. All samples were analyzed in triplicates, and heat-treated samples were used as negative control.

Telomere length

To investigate the length of the telomeres, DNA was isolated with Qiagen DNeasy Blood & Tissue Kit (Qiagen AB) according to the manufacturer's protocol from both hMSCs

Table 1C. Microarray Results of 30 Selected Genes Underexpressed in Human Embryonic Stem Cells Compared with Differentiated Cell Types

Gene name	*Gene abbreviation*	*FC hES-MP vs. hESCs*	p	*FC hES-MP vs. hMSCs*	p
Actin, alpha 2, smooth muscle, aorta	*ACTA2*	3.8	0.0612	0.1	0.2604
Bone morphogenetic protein 1	*BMP1*	1.8	0.1805	–1.4	0.0968
Bone morphogenetic protein 4	*BMP4*	**–5.1**	0.0193	1.1	0.2625
CD47 molecule	*CD47*	**6.7**	0.0013	0.7	0.1303
Cyclin-dependent kinase inhibitor 1A	*CDKN1A*	9.7	0.4477	0.1	0.0305
Collagen, type XI, alpha 1	*COLIIA1*	**10.4**	0.0000	–0.5	0.4890
Collagen, type I, alpha 1	*COLIA1*	**18.0**	0.0620	–0.8	0.4615
Collagen, type I, alpha 2	*COLIA2*	**21.8**	0.0000	–1.7	0.0443
Collagen, type II alpha 1	*COL2A1*	–4.6	0.1311	–0.6	0.0324
Collagen, type III, alpha 1	*COL3A1*	**21.2**	0.0004	**–7.6**	0.0001
Collagen, type V alpha 1	*COL5A1*	**17.0**	0.0000	–2.8	0.0177
Collagen, type V alpha 2	*COL5A2*	**18.3**	0.0000	–1.9	0.0116
Collagen, type VI, alpha 3	*COL6A3*	**67.5**	0.0000	**–3.7**	0.0075
Cystatin C	*CST3*	–1.2	0.6826	**–9.8**	0.0000
Chemokine (C-X-C motif) ligand 14	*CXCL14*	–2.1	0.0049	1.6	0.1708
Decorin	*DCN*	**5.7**	0.0302	**–51.8**	0.0114
Heart and neural crest derivatives 1	*HAND1*	–1.5	0.2841	1.0	0.9200
Insulin-like growth factor 2	*IGF2*	3.5	0.1890	**–4.8**	0.0366
Insulin-like growth factor binding protein 3	*IGFBP3*	**7.1**	0.0000	–1.8	0.2155
Insulin-like growth factor binding protein 7	*IGFBP7*	**282.2**	0.0000	–1.0	0.9241
Interleukin 6 signal transducer	*IL6ST*	**7.2**	0.0009	–1.2	0.2669
Keratin 18	*KRT18*	–1.4	0.2668	**15.0**	0.0000
Keratin 19	*KRT19*	2.2	0.1547	1.6	0.3836
Keratin 7	*KRT7*	0.2	0.2820	–1.5	0.1050
Keratin 8	*KRT8*	–2.5	0.0403	**4.3**	0.0004
Lumican	*LUM*	5.0	0.1418	**–17.4**	0.0000
N-mye downstream regulated gene 1	*NDRG1*	**4.5**	0.0000	–2.5	0.0008
Procollagen-proline	*P4HA2*	**12.1**	0.0000	–2.5	0.0000
Rho-related BTB domain containing 3	*RHOBTB3*	**4.1**	0.0009	–1.9	0.0425
Osteonectin	*SPARC*	**5.8**	0.0000	–1.3	0.1162

Genes significantly regulated are in boldface.

and hES-MPs at low and high passage. After isolation of DNA, the length of the telomeres was measured using the *TeloTAGGG* Telomere Length Assay kit (Roche Diagnostics Scandinavia AB) according to the protocol provided by the manufacturer.

Results

Flow cytometry analysis of hMSCs

Flow cytometry analysis was used to evaluate the enrichment of a homogenous population of hMSCs, demonstrating that 96% ± 2% of the cells were CD166 + /CD45 − and 94% ± 1% of the cells were CD105+/CD34−.

Cell morphology

While hESCs (Fig. 1A) exhibited their typical morphology and characteristic growth in colonies, the hES-MPs (Fig. 1B) displayed a fibroblast-like morphology characteristic of hMSCs (Fig. 1C).

Global gene expression comparison

Scatter plot analysis of the microarray data for each pairwise comparison showed that hES-MPs and hMSCs display a more narrow spatial distribution of gene expression, with 90% of the genes displaying an FC $\leq$3 (Fig. 2A, D). Results from the other two comparisons (hESCs vs. hES-MPs and hESCs vs. hMSCs) showed larger transcriptional differences with 25% or more of the genes with an FC $\geq$3 (Fig. 2B–D). The Spearman correlation coefficients demonstrated a higher correlation between hES-MPs and hMSCs (0.92) than between hESCs vs. hES-MPs (0.83) and hESCs vs. hMSCs (0.79) (Fig. 2D). Hierarchial clustering of 447 genes with an FC $\geq$20 resulted in three main groups—hESCs, hES-MPs, and hMSCs (Fig. 2E). This analysis further demonstrates that the hES-MPs and the hMSCs display a more similar expression pattern than hES-MP compared with hESCs.

In Table 1A, the expression levels of 40 genes known to be specifically expressed in hESCs is shown. Out of these genes, 27 genes were significantly downregulated during hES-MP derivation and most of the genes (32 out of 40) displayed a transcription level similar to hMSCs. Among these genes, several genes involved in the maintenance of pluripotency (*POU5F1*, *NANOG*, *ZIC3*, *TDGF1*, and *LIN28*) significantly decreased in expression at least 50 times during hES-MP derivation; with the exception of *NANOG*, no significant differences in expression of these genes were detected between hES-MPs and hMSCs. None of the markers for hESCs increased in expression during hES-MP derivation. Three genes (*BRRN1*, *FLJ20105*, and *HELLS*) displayed an at least

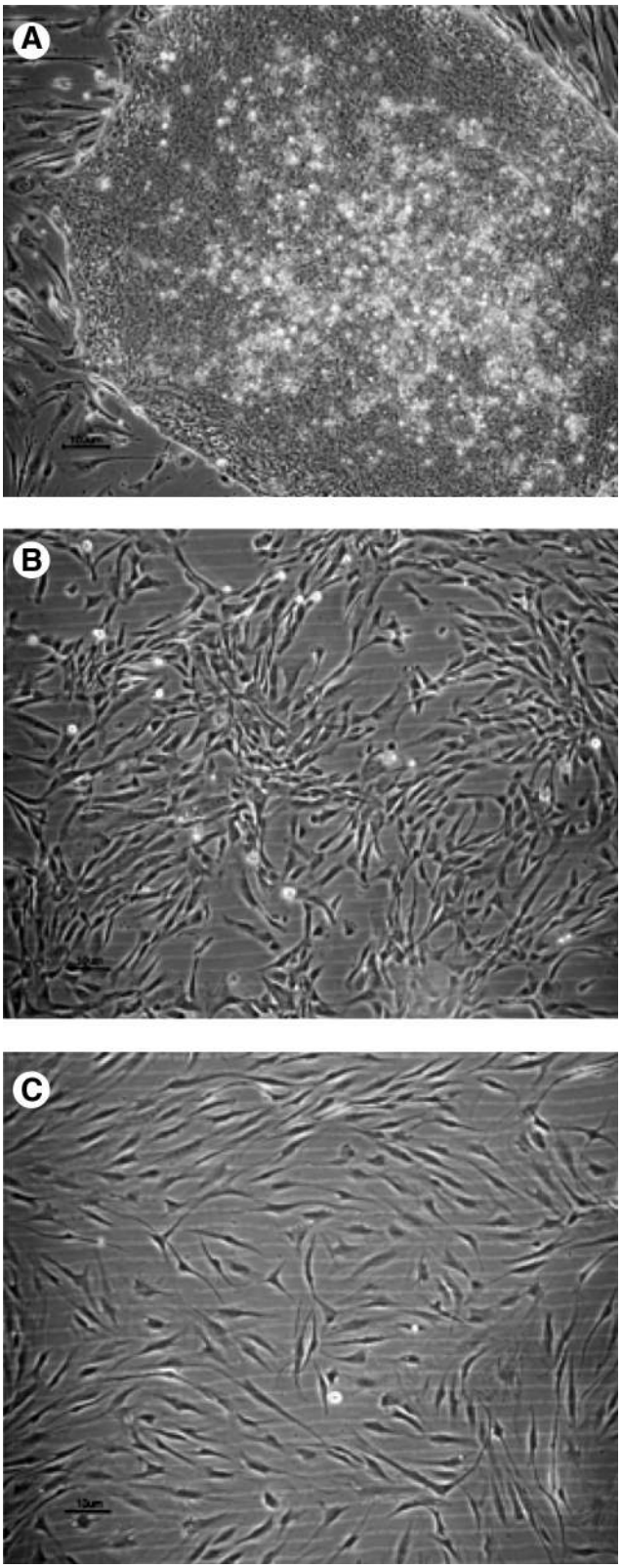

FIG. 1. Light micrographs showing human embryonic stem cells (hESCs) (**A**) growing on a mouse embryonic fibroblast feeder layer (scale bar = 100 μm), and hESC-derived mesodermal progenitors (hES-MPs) (**B**) and human mesenchymal stem cells (hMSCs) (**C**) expanded on tissue culture plastic (scale bar = 10 μm).

10-fold higher expression in hES-MPs compared with hMSCs, whereas *MCM10*, *CDC25A*, and *ORC1L* showed a 9.7-fold, 6.1-fold, and 4.6-fold higher expression in hES-MPs compared with hMSCs.

Analyzing expression of 48 genes known to be overexpressed in hESCs compared with differentiated cell types demonstrated that 39 genes decreased in transcription during hES-MP formation (Table 1B). Within this group of genes, some additional genes of importance for pluripotency were detected as significantly downregulated during hES-MP derivation, including *LEFTY1* and *SOX2*. None of the 48 genes known to be overexpressed in hESCs compared with differentiated cell types displayed higher expression in hES-MPs compared with hESCs. Genes differentially expressed between hES-MPs and hMSCs include *MCM5*, which had 9.2-fold higher expression in hES-MPs compared with hMSCs, and *PLA2G16*, displaying a higher expression in hMSCs.

Of the 30 selected genes known to be underexpressed in hESCs compared with differentiated cell types, 15 genes were induced during hES-MP derivation (Table 1C). Some of these genes include genes encoding mesodermal extracellular matrix components (*COL1A1*, *COL1A2*, *COL2A1*, *COL3A1*, *COL5A1*, *COL5A2*, *COL11A1*, and *COL6A3*) (Table 1C). The majority of these genes were induced to the same level as seen in hMSCs. On the other hand, genes encoding markers for ectodemal tissues, such as keratins (*KRT18*, *KRT19*, *KRT7*, and *KRT8*) were not induced during the process of hES-MP formation.

In Table 2 (A, B), the 15 most up- and down-regulated genes per each of the 5 categories described above are listed, if existing. Several genes encoding transcription factors displayed a decreased transcription during hES-MP derivation (*SIX1*, *PPRX1*, *NR2F2*, *BNC1*, *RUNX2*, and *BCOR*). The hMSCs displayed the highest expression level of the *HOX* genes (*HOXA9*, *HOXA10*, *HOXC6*, and *HOXC10*), their downstream mediator *EMX2* and *IRX3*, as well as *FOS* genes (*FOS* and *FOSB*). Studying genes encoding extracellular matrix components induced during hES-MP derivation, we added the following genes to the results described above: *COL1A2*, *COL6A2*, *COL6A*, *BGN*, *MFAP5*, *FN1*, and *FBN1*. Several genes encoding matrix proteins were thus induced during hES-MP formation; in fact, the only gene in this category that was found to have higher expression in hESCs than in hES-MPs and hMSCs was *LAMA1*.

For the membrane receptor category, essential receptors for mesodermal differentiation, such as *TGFRB2* and *BMPR2*, are shown to be expressed to a greater extent in hES-MPs and hMSCs compared with hESCs. Finally, genes encoding cell adhesion molecules, including the hMSCs markers *CD44*, *CD58*, *CD47*, and *CD166* (*ALCAM*), were significantly induced during hES-MP derivation to a level similar to hMSCs.

In total, 9 hubs were identified among the genes induced by hES-MP derivation (*PLAU*, *THBS1*, *FN1*, *COL1A1*, *COL1A2*, *MFS2*, *CD44*, *CDKN2A*, and *CAV1*) (Fig. 3A). Only one hub, *EWSR1*, was identified among the genes repressed during this process (Fig. 3B). Hub genes with higher expression in hES-MPs compared with hMSCs include several genes composing the spindle assembly checkpoint (*CDC20*, *AURKA*, *AURKB*, *BUB1B*, *NDC20*, *MAD2*, *ERCC6L*, *NUF2*, *CENPA*, *AP14*, *SPC24*, *D40*, *SPC25*, *CENPM*, *MLF1IP*, *ZWINT*, *CENPF*, *CDCA8*, *NEK2*, and

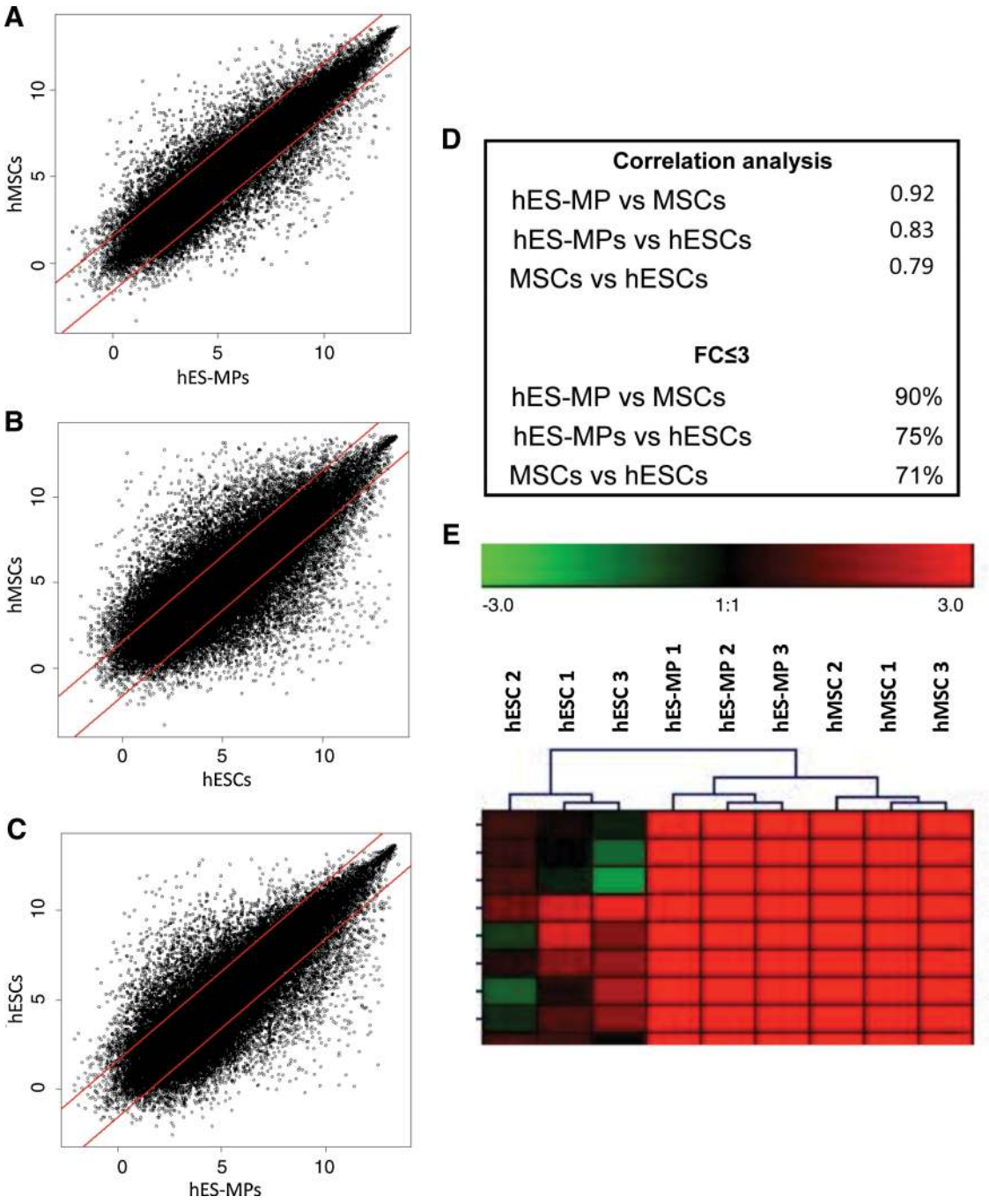

FIG. 2. Scatter plots (**A–C**), where genes within the lines indicate a fold change (FC) of less than ± 3. Summary of the scatter plots and Spearman correlation analysis (**D**). Hierarchical clustering of genes with an FC ≥ 20 (**E**). Color images available online at www.liebertonline.com/ten.

CCNB1) (Fig. 3C). Only one hub gene, *JUN*, was identified among the genes with higher expression in hMSCs than hES-MPs (Fig. 3D).

Real-time PCR

Microarray results for *TDGF*, *TGF-β2R*, *RUNX2*, *COL1A1*, *LHX8*, and *BMP2R* were verified using real-time PCR, which corroborated the microarray results in all cases except for *BMP2R*, in which no significant differences could be detected between the three different cell types studied (Fig. 4A–F).

Flow cytometry

The flow cytometry analysis confirmed the microarray results for adhesion proteins characteristic for hMSCs (CD44, CD58, CD166, and CD47), demonstrating that the undifferentiated hESCs displayed significantly lower expression of these four markers compared with the hMSCs and hES-MPs,

Table 2A. Microarray Results for the Most Differentially Regulated Genes Comparing Human Embryonic Stem Cells and Human Embryonic Stem Cell–Derived Mesodermal Progenitors

Gene name	*Gene abbreviation*	*Probe ID*	*FC hES-MPs vs. hESC*	p	*FC hES-MPs vs. hMSCs*	p
Transcription factors						
SIX homeobox 1	*SIXI*	228347_at	364.8	0	0.1	0.0002
Paired related homeobox 1	*PRRX1*	226695_at	317.6	0	1.9	0.0513
Nuclear receptor subfamily 2, group F, member 2	*NR2F2*	215073_s_at	197.0	0	6.9	0
Basunuclan 1	*BNC1*	1552487_a_at	151.6	0	−1.2	0.4694
Distal-less homeobox 1	*DLX1*	242138_at	104.8	0	15.3	0
LIM homeobox 8	*LHX8*	1569469_a_at	81.9	0	95.5	0.0040
Forkhead box D1	*FOXD1*	206307_s_at	69.7	0	1.9	0.0469
Zinc finger E-box binding homeobox 1	*ZEB1*	212764_at	68.6	0	1.3	0.1708
Distal-less homeobox 2	*DLX2*	207147_at	56.6	0	17.3	0
Twist homolog 1	*TWIST1*	213943_at	42.2	0	−2.1	0.0987
Neuronal PAS domain protein 2	*NPAS2*	39549_at	40.9	0	1.2	0.1158
Runt related transcription factor 2	*RUNX2*	232231_at	38.8	0	−2.1	0.1482
Nuclear factor I/X	*NFIX*	237400_at	31.3	0	−2.3	0
Teashirt zinc finger homeobox 1	*TSH21*	223282_at	26.0	0	−1.3	0.0224
Homeobox A3	*HOXA3*	235521_at	25.8	0	−1.7	0.0052
Hary and enhancer of split 6	*HES6*	226446_at	−21.6	0	−1.1	0.1590
BCL6 co-repressor	*BCOR*	223916_s_at	−34.3	0	−2.1	0.2558
Zinc finger protein 165	*ZNF165*	206683_at	−37.0	0	−3.6	0.0691
Nuclear receptor subfamily 6, group A. member 1	*NR6A1*	227494_at	−41.9	0	−1.0	0.3698
SRY (sex determining region Y) box 2	*SOX2*	228038_at	−52.8	0	10.7	0.0052
SRY (sex determining region Y) box 4	*SOX4*	213668_s_at	−55.3	0	−3.4	0.1217
Forkhead box O1	*FOXO1*	202724_s_at	−58.4	0	−5.2	0.0715
Forkhead box H1	*FOXH1*	231407_s_at	−62.5	0	1.5	0.2629
HESX homeobox 1	*HESX1*	211207_at	−84.4	0	−4.8	0.0512
POU class 5 homeobox 1 pseudogene 3	*POUSF1*	208286_x_at	−445.7	0	1.0	1.0000
Zinc finger and SCAN domain containing 10	*ZSCAN10*	1553874_a_at	−702.1	0	1.1	0.5828
OTX2	*OTX2*	242138_at	−877.3	0	1.2	0.7673
POU class 5 homeobox 1 pseudogene 3	*POUSF1P3*	210265_x_at	−1064.2	0	−2.2	0.0005
POU class 5 homeobox 1 pseudogene 4	*POUSF1P4*	210905_x_at	−1140.6	0	−1.1	0.5877
Nanog	*NANOG*	220184_at	−1482	0	−4.3	0.0001
Membrane receptors						
Discoidin domain receptor tyrosine kinase 2	*DDR2*	225442_at	57.0	0	−2.4	0
Transforming growth factor receptor beta 2	*TGFBR2*	208944_at	25.8	0	1.0	0.9020
Thrombomodulin	*THBD*	203887_s_at	18.4	0.0023	4.0	0.1380
AXL receptor tyrosine kinase	*AXL*	202686_s_at	17.5	0	1.2	0.4780
Protein tyrosine phosphatase, receptor type, B	*PTPRB*	230250_at	16.2	0.0013	4.2	0.0600
Tumor necrosis factor receptor superfamily, member 10d	*TNFRSF10D*	227345_at	15.3	0	3.5	0.0180
Interleukin 1 receptor 1	*IL1R1*	202948_at	14.5	0	−3.2	0.0010
Platelet-derived growth factor receptor, alpha polypeptide	*PDGFRA*	203131_at	13.7	0.0002	−1.5	0.2510
Bone morphogenetic protein receptor, type 2	*BMPR2*	231873_at	10.2	0	1.6	0.0190

Toll-like receptor adaptor molecule 2	*TICAM2*	228234_at	10.1	0.0003	−1.7	0.0060
Fas (TNF receptor superfamily, member 6)	*FAS*	215719_x_at	7.9	0	−1.6	0.1500
Epidermal growth factor receptor	*EGFR*	201983_s_at	4.8	0.0017	−1.8	0.0030
Leptin receptor	*LEPR*	209894_at	4.2	0	−5.3	0
Protein tyrosine phosphatase, receptor type, M	*PTPRM*	1555579_s_at	4.1	0.0001	−2.3	0.0010
Leptin receptor overlapping transcript	*LEPROT*	202378_s_at	3.9	0.0002	−1.6	0.0030
Low density lipoprotein receptor related protein 8	*LRP8*	208433_s_at	−3.1	0.0001	2.0	0.0780
Bone morphogenetic protein receptor, type 1A	*BMPR1A*	204832_s_at	−3.4	0	1.3	0
TYRO3 protein tyrosine kinase	*TYRO3*	211432_s_at	−4.7	0	−1.2	0.3500
Insulin-like growth factor 1 receptor	*IGF1R*	203628_at	−5.6	0	−1.4	0.0760
Fibroblast growth factor receptor substrate 2	*FRS2*	221308_at	−10.0	0.0059	−1.1	0.6390
Protein tyrosine phosphatase, receptor type, D	*PTPRD*	213362_at	−13.9	0.0328	−1.1	0.9270
Activim A receptor, type IIB	*ACVR2B*	236126_at	−15.6	0	1.2	0.1910
Receptor tyrosine kinase-like orphan receptor 1	*ROR1*	232060_at	−19.5	0.0100	−8.4	0.0010
Claudin 3	*CLDN3*	203953_s_at	−37.3	0	1.1	0.4970
EPH receptor A1	*EPHA1*	205977_s_at	−44.2	0	1.1	0.4980
Plexin B1	*PLXNB1*	215807_s_at	−54.9	0	−1.3	0.0020
Protein tyrosine phosphatase, receptor-type, Z polypeptide 1	*PTPRZ1*	204469_at	−76.4	0	4.6	0.0210
Growth factors						
Fibroblast growth factor 5	*FGF5*	210310_s_at	197.0	0	133.0	0
Epiregulin	*EREG*	205767_at	182.4	0	5.7	0.0068
Latent transforming growth factor beta binding protein 2	*LTBP2*	223690_at	25.6	0	−4.7	0.0076
HtrA serine peptidase 1	*HTRA1*	201185_at	11.9	0.0068	−2.4	0.0435
Growth and differentiation factor 5	*GDF15*	221577_x_at	7.2	0.0025	−17.7	0
Heparin-binding EGF like growth factor	*HBEGF*	203821_at	6.6	0	5.7	0
Insulin receptor substrate 1	*IRS1*	204686_at	3.4	0.0006	1.4	0.1238
Left-right determination factor 1	*LEFTY1*	206268_at	−14.3	0.0006	−1.1	0.4192
Teratin carcinoma derived growth factor 1	*TDGF1*	206286_s_at	−315.2	0	1.5	0.5798
Extracellular matrix components						
Biglycan	*BGN*	213905_x_at	161.3	0	−4.7	0
Microfibrillar associated protein 5	*MFAP5*	213764_s_at	132.0	0.0014	7.0	0.0043
Laminin, alpha 4	*LAMA4*	202202_s_at	74.1	0	−3.2	0.0070
Collagen, type 1, alpha 1	*COL1A1*	202311_s_at	50.4	0	−1.1	0.9130
Fibrillin 1	*FBN1*	202765_s_at	50.4	0.0001	−3.1	0
Collagen, type III, alpha 1	*COL3A1*	211161_s_at	42.2	0.0006	−5.5	0.0002
Collagen type I, alpha 2	*COL1A2*	229218_at	22.8	0	−2.3	0.0010
Collagen, type V, alpha 1	*COL5A1*	212489_at	21.4	0	−2.4	0.0219
Fibronectin 1	*FN1*	214702_at	19.4	0.0006	−13.7	0
Collagen, type V, alpha 2	*COL5A2*	221730_at	18.8	0	−2.2	0.0037
Collagen type XI, alpha 1	*COL11A1*	229271_x_at	13.4	0	1.1	0.6640
Collagen, type VI, alpha 2	*COL6A2*	209156_s_at	8.8	0.0001	−3.6	0
Nidogen I	*NID1*	202007_at	6.6	0	−1.8	0.0269
Collagen, type VI, alpha 1	*COL6A1*	213428_s_at	4.6	0	−2.0	0.0014
Laminin, gamma I	*LAMC1*	*200771_at*	3.3	0	−1.4	0.0780
Laminin alpha 1	*LAMA1*	227048_at	−15.0	0	−4.5	0.0002

(*continued*)

Table 2A. (Continued)

Gene name	*Gene abbreviation*	*Probe ID*	*FC hES-MPs vs. hESC*	p	*FC hES-MPs vs. hMSCs*	p
Cell adhesion						
CD44	*CD44*	212063_at	74.7	0	1.1	0.4800
Cadherin 13, H-cadherin	*CDH13*	204726_at	70.2	0	1.7	0.3800
Discoidim domain receptor tyrosine kinase 2	*DDR2*	225442_at	57.0	0	−2.4	0
CD58	*CD58*	216322_at	50.4	0	−1.3	0.0850
ADAM metallopeptidase domain 12	*ADAM12*	226777_at	31.8	0.0026	−1.1	0.8770
Integrin, alpha 2 (CD49B	*ITGA2*	227314_at	30.3	0	5.1	0.0060
Neurotrimin	*HNT*	227566_at	15.9	0	−1.2	0.5830
CD477 Check	*CD47*	226016_at	14.5	0	1.7	0.0110
Neural cell adhesion molecule 2	*NCAM2*	205669_at	11.8	0.0002	1.3	0.4500
CD99	*CD99*	201028_s_at	11.7	0	−1.4	0.0170
Activated leukocyte cell adhesion molecule 166	*ALCAM*	201951_at	9.8	0	−1.1	0.4700
Claudin 1	*CLDN 1*	222549_at	8.4	0.0035	2.9	0.0170
RGM domain faculty, member B	*RGMB*	227340_s_at	7.9	0.0006	4.4	0
Integrin, alpha 3 (antigen CD49C	*ITGA3*	201474_s_at	6.9	0	1.4	0.0120
CD151	*CD151*	204306_s_at	6.3	0	−1.0	0.9080
Trophinin	*TRO*	211700_s_at	−3.1	0.0255	1.3	0.3020
Claudin 10	*CLDN10*	205328_at	−8.4	0	1.4	0.1290
Protocadherin 7	*PCDH7*	205535_s_at	−9.1	0.0190	−1.6	0.5430
Claudin 3	*CLDN3*	203953_s_at	−37.3	0	1.1	0.4970
Protocadheria 8	*PCDH8*	206935_at	−127.0	0	1.4	0.6360
Claudin 6	*CLDN6*	237810_at	−364.8	0.0001	2.4	0.0150

FC, fold change; hESC, human embryonic stem cell; hES-MP, hESC-derived mesodermal progenitor; hMSC, human mesenchymal stem cell.

Table 2B. Microarray Results for the Most Differentially Regulated Genes Comparing Human Mesenchymal Stem Cells and Human Embryonic Stem Cell–Derived Mesodermal Progenitors

Gene name	*Gene abbreviation*	*Probe ID*	*FC hES-MPs vs. hMSC*	p	*FC hEs-MPs vs. hESCs*	p
Transcription factors						
LIM homeobox 8	*LHX8*	1569469_a_at	95.5	0	81.9	0.0050
Transcription factor AP-2 alpha	*TFAP2A*	204653_at	21.1	0	10.8	0.0005
Sal-like 1	*SALL1*	229273_at	18.1	0.0105	−2.3	0.0432
Distal-less homeobox 2	*DLX2*	207147_at	17.3	0	56.6	0
Msh homeobox 1	*MSX1*	205932_s_at	17.0	0	17.3	0.0073
Forkhead box F1	*FOXF1*	205935_at	15.5	0	18.5	0
Distal-less homeobox 1	*DLX1*	242138_at	15.3	0	104.8	0
Leucine zipper, putative tumor suppressor 1	*LZTS1*	47550_at	14.0	0.0154	1.5	0.2533
Paired box 3	*PAX3*	231666_at	10.3	0.0083	6.2	0.1352
Hematopoietically expressed homeobox	*HHEX*	215933_s_at	8.9	0	13.8	0
SIX homeobox 1	*SIX1*	205817_at	8.4	0	54.4	0
Zinc finger protein 367	*ZNF367*	229551_x_at	7.6	0	−2.2	0.1852
Nuclear factor (erythroid-derived 2)-like 3	*NFE2L3*	204702_s_at	4.4	0.0109	−1.6	0.0696
Myelin expression factor 2	*MYEF2*	222772_at	4.3	0.0008	1.1	0.6430
Transducin-like enhancer of split 1	*TLE1*	228284_at	4.3	0	−2.7	0.0037
Runt-related transcription factor 2	*RUNX2*	236859_at	−10.2	0.0001	2.5	0.3904
Activating transcription factor 3	*ATF3*	202672_s_at	−11.1	0	−9.8	0.0008
Kruppel-like factor 15	*KLF15*	231015_at	−15.5	0	−11.8	0.0006
Zinc finger protein 37A	*ZNF37A*	228711_at	−15.5	0.0012	−1.4	0.7851
Growth and differentiation factor 15	*GDF15*	221577_x_at	−17.7	0	7.2	0.0025
Kruppel-like factor 9	*KLF9*	203543_s_at	−18.7	0	3.9	0.0022
Empty spiracles homeobox 2	*EMX2*	221950_at	−21.8	0	−1.1	0.9197
Homeobox C10	*HOXC10*	218959_at	−28.3	0	−1.0	0.8273
Nuclear receptor subfamily 1, group D, member 1	*NRID1*	204760_s_at	−29.4	0	−2.7	0.0069
V-fos FBJ murine osteosarcoma viral oncogene homolog	*FOS*	209189_at	−34.6	0.0001	−38.2	0.0298
FBJ murine osteosarcoma viral oncogene homolog B	*FOSB*	202768_at	−36.5	0	−26.2	0.0015
Iroquois homeobox 3	*IRX3*	229638_at	−48.9	0	1.1	0.8405
Homeobox C6	*HOXC6*	206858_s_at	−79.4	0	2.4	0.0650
Homeobox A10	*HOXA10*	213150_at	−82.5	0	2.3	0.3328
Homeobox A9	*HOXA9*	209905_at	−147.0	0	−2.0	0.0031
Membrane receptors						
Protein tyrosine phosphatase, receptor type, F	*PTPRF*	200636_s_at	5.0	0	−1.1	0.8129
Tumor necrosis factor receptor superfamily, member 10d	*TNFRSF10*	210654_at	5.0	0.0103	2.7	0.0002
LDLR	*LDLR*	202068_s_at	3.9	0.0001	1.2	0.5472
Tumor necrosis factor receptor superfamily, member 25	*TNFRSF25*	219423_x_at	2.5	0.0013	2.5	0
Fas (TNF receptor superfamily, member 6)	*FAS*	204780_s_at	−2.1	0.0008	7.1	0.0001
Activin A receptor, type 1	*ACVR1*	203935_at	−2.3	0	2.0	0
Protein tyrosine phosphatase, receptor type, M	*PTPRM*	1555579_s_at	−2.3	0.0007	4.1	0.0001
Protein tyrosine phosphatase, receptor type, G	*PTPRG*	204944_at	−2.6	0	−2.0	0.0435
ECF-containing fibulin like extracellular matrix protein 2	*EFEMP2*	209356_x_at	−2.8	0.0005	9.0	0.0008
Interleukin 1 receptor 1	*IL1R1*	202948_at	−3.2	0.0014	14.5	0
Natnuretic peptide receptor Biguanylate cyclase B	*NPR1*	204310_s_at	−3.4	0	1.9	0.0058
Discoidin domain receptor tyrosine kinase 2	*DDR2*	205168_at	−4.3	0.0001	7.4	0.0003

(*continued*)

Table 2B. (Continued)

Gene name	*Gene abbreviation*	*Probe ID*	*FC hES-MPs vs. hMSC*	p	*FC hEs-MPs vs. hESCs*	p
Insulin receptor	*INSR*	226216_at	−4.8	0.0001	−2.3	0.2379
Docking protein 5	*DOK5*	214844_s_at	−4.9	0.0041	−3.2	0.0086
Leptin receptor	*LEPR*	209894_at	−5.3	0.0003	4.2	0
Receptor tyrosine kinase-like orphan receptor 1	*ROR1*	232060_at	−8.4	0.0007	−19.5	0.0100
Toll-like receptor 3	*TLR3*	206271_at	−8.8	0	2.2	0.1322
Lymphotoxin beta receptor (TNFR superfamily, member 3)	*LTBR*	203005_at	−12.0	0	1.6	0.3881
EPH receptor A1	*EPHA3*	206070_s_at	−21.4	0	−3.9	0.2093
Growth factors						
Fibroblast growth factor 5	*FGF5*	210310_s_at	133.0	0	197.0	0
Epiregulin	*EREG*	205767_at	5.7	0.0068	182.4	0
Heparin-binding EGF-like growth factor	*HBEGF*	203821_at	5.7	0	6.6	0
Activin A receptor, type 1	*ACVR1*	203935_at	−2.3	0	2.0	0
Latent transforming growth factor beta binding protein 2	*LTBP2*	204682_at	−6.1	0	12.5	0.0003
Growth and differentiation factor 5	*CDF15*	221577_x_at	−17.7	0	7.2	0.0025
Extracellular matrix components						
Microfibrillar associated protein 5	*MFAP5*	213764_s_at	7.0	0.0015	132	0.0014
Collagen, type IV, alpha 6	*COL4A6*	213992_at	4.6	0.0007	−2.7	0.0098
Laminin, gamma 1	*LAMC1*	200770_s_at	−2.7	0.0029	2.9	0
Fibrillin 1	*FBN1*	202765_s_at	−3.1	0.0002	50.4	0.0001
Collagen, type VI, alpha 1	*COL6A1*	212091_s_at	−3.1	0.0011	2.0	0.0028
Collagen, type V, alpha 1	*COL5A1*	203325_s_at	−3.3	0.0045	9.6	0
Collagen, type V, alpha 2	*COL6A2*	209156_s_at	−3.6	0.0020	8.8	0.0001
Biglycan	*BGN*	201262_s_at	−4.3	0	1.9	0.0058
Matrilin 2	*MATN2*	202350_s_at	−4.4	0.0002	−2.5	0.0004
Laminin, alpha 1	*LAMA1*	227048_at	−4.5	0.0074	−15	0
Collagen, type III, alpha 1	*COL3A1*	201852_x_at	−8.1	0.0002	16.2	0
Fibronectin 1	*FN1*	214702_at	−13.7	0	19.4	0.0006
Collagen, type XIV, alpha 1	*COL14A1*	212865_s_at	−15.6	0	−1.9	0.0185
Lumican	*LUM*	201744_s_at	−17.4	0	5.0	0.1156
Collagen, type XV, alpha 1	*COL15A1*	203477_at	−19.5	0.0005	1.3	0.8194
Chitinase 3-like 1 (cartilage glycoprotein-39)	*CHI3L1*	209395_at	−151.6	0	−1.6	0.1956
Cell adhesion						
Protocadherin alpha 1	*PCDHA1*	223435_s_at	20.2	0.0056	−1.7	0.1871
Protocadherin beta 2	*PCDHB2*	231725_at	13.1	0	1.3	0.5476
Cadherin 6, type 2, K-cadherin	*CDH6*	214803_at	11.8	0.0007	27.2	0.0041
Integrin alpha 2 (CD49B	*ITGA2*	227314_at	5.1	0.0058	30.3	0
Protein tyrosine phosphatase, receptor type, F	*PTPRF*	200636_s_at	5.0	0	−1.1	0.8129
Pinin, dexosome associated protein	*PNN*	212037_at	4.7	0	−2.9	0
CD9	*CD9*	201005_at	4.5	0	1.4	0.2742
Melanoma cell adhesion molecule	*MCAM*	211042_x_at	3.5	0	−1.5	0.1037
Catenin (cadherin-associated protein), beta 1	*CTNNB1*	223679_at	−2.7	0.0005	−3.0	0.0005
Discoidin domain receptor Tyrosine kinase 2	*DDR2*	205168_at	−4.3	0.0001	7.4	0.0003
Neuronal cell adhesion molecule	*NRCAM*	204105_s_at	−5.4	0.0006	−2.5	0.2925
Vascular cell adhesion molecule 1	*VCAM1*	2038685_s_at	−11.2	0	2.3	0.1696
CD97	*CD97*	202910_s_at	−12.5	0	2.6	0.0945

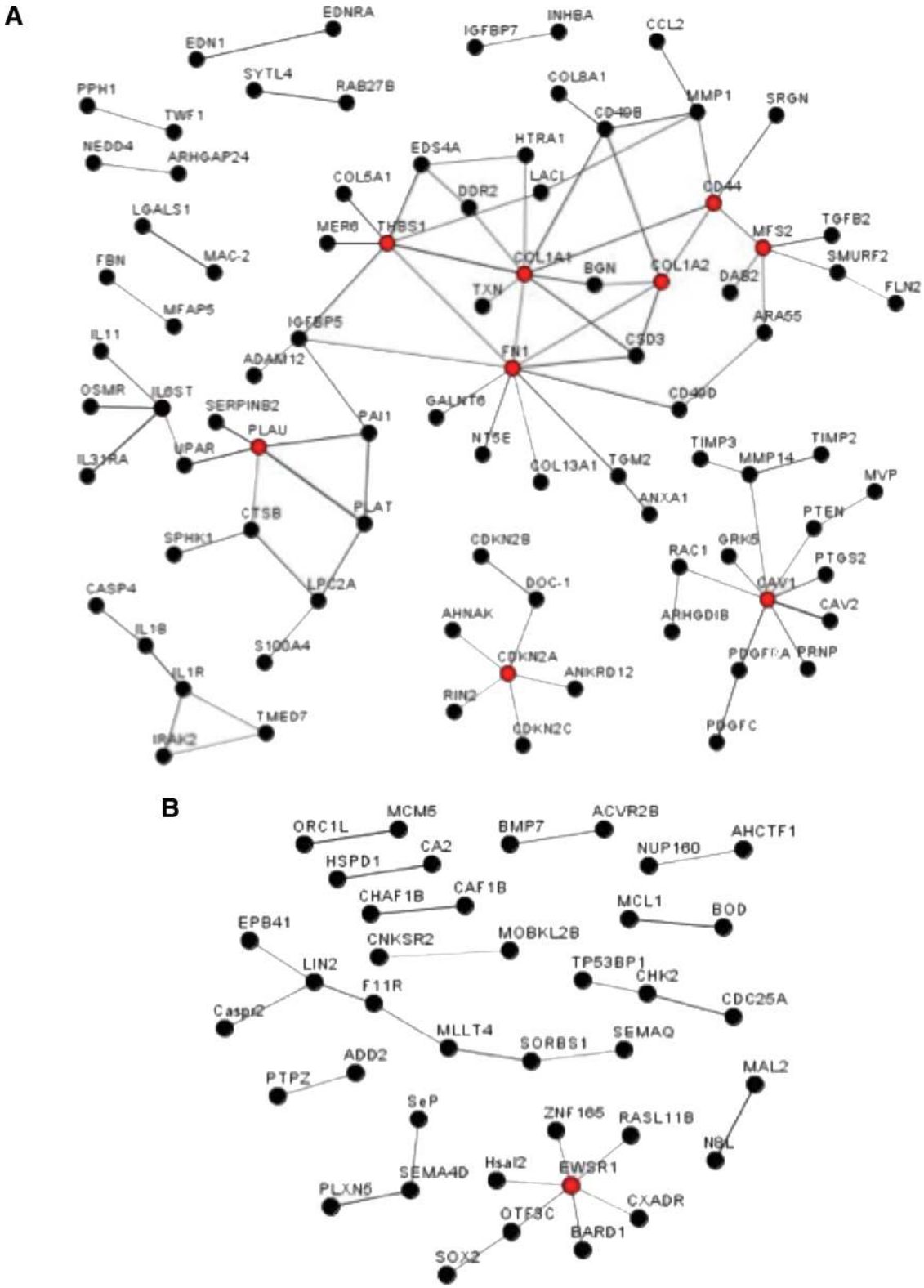

FIG. 3. Hub protein network of genes induced (**A**) and repressed (**B**) during hES-MPs derivation, as well as genes with an increased (**C**) and decreased (**D**) expression in hES-MPs compared with hMSCs with at least a 10-FC in expression. Proteins are identified as hubs if they have at least five experimentally determined protein interactions among the products of the up-regulated genes. Color images available online at www.liebertonline.com/ten.

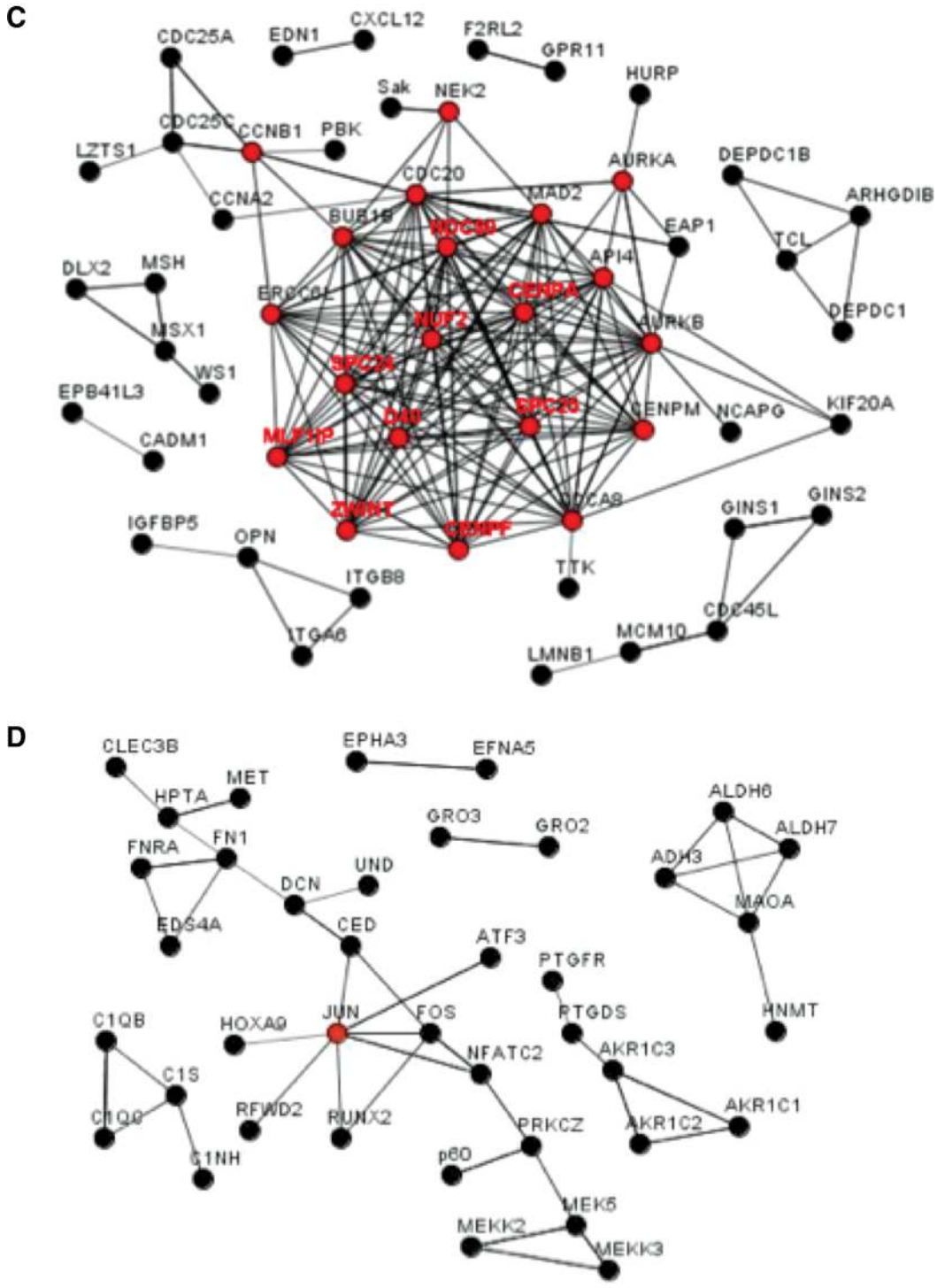

FIG. 3. (Continued).

which showed a comparable expression for all of the markers studied (Fig. 4G–J).

Immunohistochemistry

Immunohistochemistry demonstrated that only hESCs were positively stained for OCT4 and NANOG as shown in Figure 4 (K, N), whereas hES-MP cells (L, O) and hMSCs (M, P) were negative for both markers.

Proliferation ability

Throughout the proliferative assay, the hES-MPs displayed a significantly higher number of cell doublings per time period compared with the hMSCs (Fig. 5A). Around passages 8–10, an initial decline in the proliferative potential of hMSCs was detected. This was followed by a more or less ceased proliferation after passage 20. The hES-MPs, on the other hand, retained their high proliferative

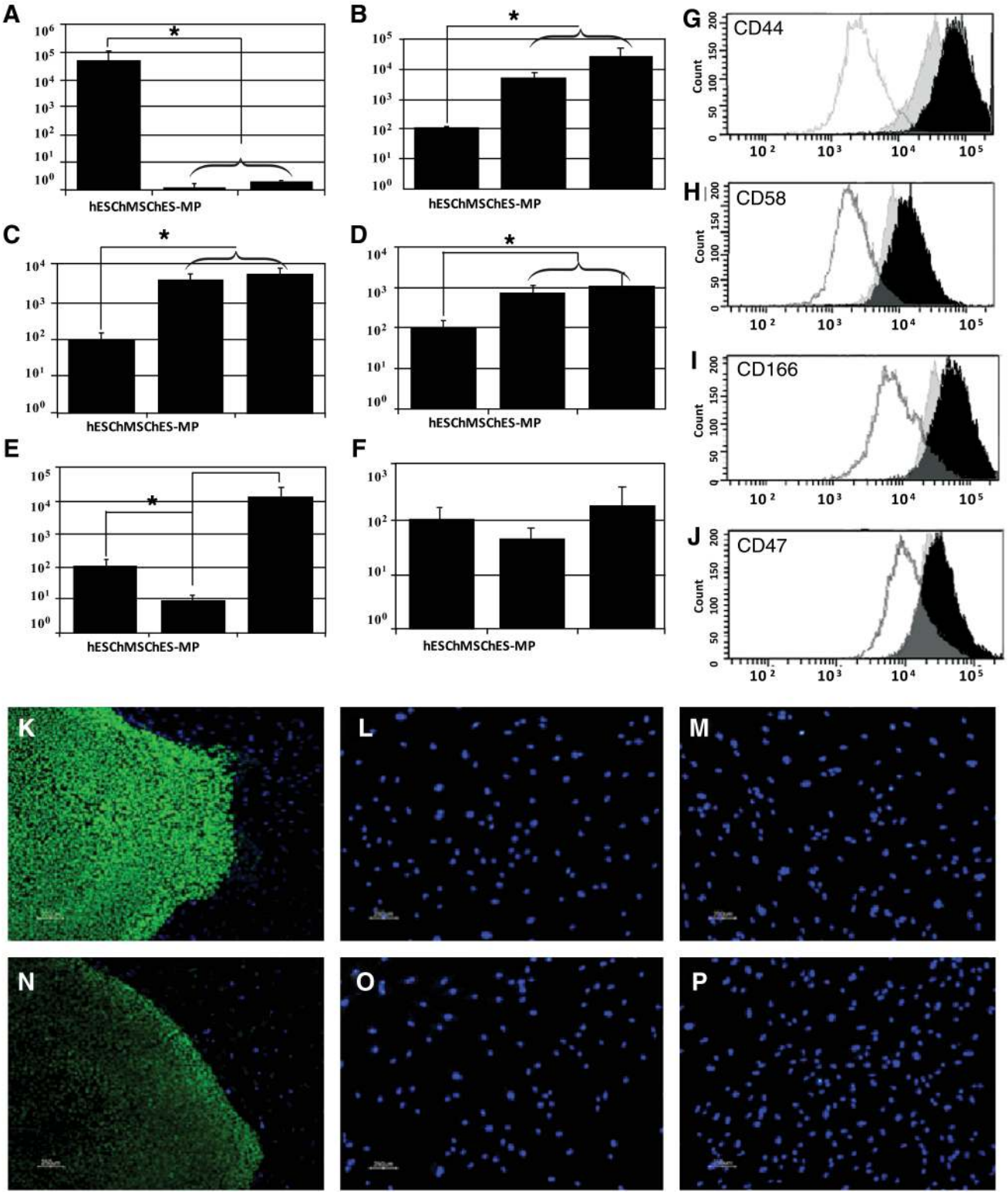

FIG. 4. Verification of microarray results using quantitative RT-polymerase chain reaction analysis for *TDGF1* (**A**), *TGF*-β2*R* (**B**), *RUNX2* (**C**), *COL1A1* (**D**), *LHX8* (**E**), and *BMP2R* (**F**) (differences were accepted to be statistically significant at $p \leq 0.05$ (*)). Flow cytometry analysis of CD44 (**G**), CD58 (**H**), CD166 (**I**), and CD47 (**J**) for hESCs (white), hES-MPs (black), and hMSCs (gray). Expression of OCT4 (**K–M**: scale bar = 250 μm) and NANOG (**N–P**: scale bar = 250 μm) in hESCs (**K, N**), hES-MPs (**L, O**), and hMSCs (**M, P**). Color images available online at www.liebertonline.com/ten.

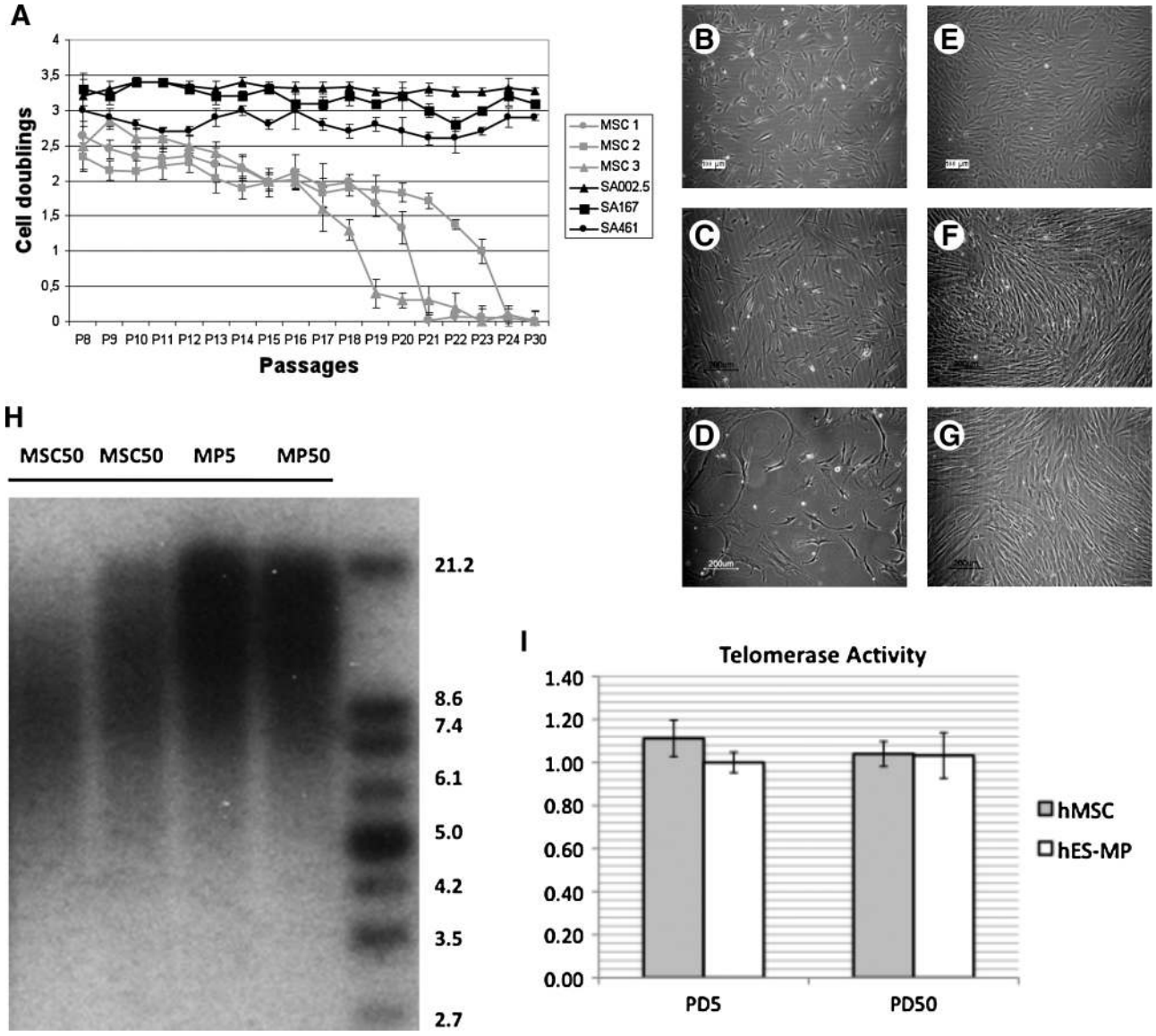

FIG. 5. Cell doublings of hMSCs and hES-MPs (**A**). Light micrographs of hMSCs (**B–D**) and hES-MPs (**E–G**) at passage 5 (**B, E**: scale bar = 100 μm), 10 (**C, F**: scale bar = 200 μm), and 20 (**D, G**: scale bar = 200 μm). Telomere length (**H**) and telomerase activity (**I**) of both cell types at population doubling 5 and 50 (PD5 and PD50).

capacity for the whole duration of the test (up to passage 30).

Telomerase activity and telomere length

Both hES-MPs and hMSCs at PD 5 and 50 showed a similar level of telomerase activity (Fig. 5I). In contrast, the telomeric repeat fragments were longer for hES-MPs compared with hMSCs at both passages investigated (Fig. 5H).

HLA expression

Flow cytometry analysis for immunological markers demonstrated that both hMSCs and hES-MPs were found to be negative for CD80 (Fig. 6A, I) and CD86 (Fig. 6B, J). Expression of these two markers was further not affected by IFN-γ treatment in either hMSCs (Fig. 6E, F) or hES-MPs (Fig. 6M, N). On the other hand, all hMSCs were positive for HLA-ABC (Fig. 6C) and about half of the hMSC population was also positive for HLA-DR (Fig. 6D). Expression of these two markers further increased after IFN-γ treatment (Fig. 6G, H). In contrast, the hES-MPs displayed somewhat lower expression of HLA-ABC compared with the hMSCs (Fig. 6K) and were negative for HLA-DR (Fig. 6L). Expression of HLA-ABC after IFN-γ treatment of hES-MPs (Fig. 6O) was similar to that of IFN-γ-treated hMSCs. A small population of hES-MPs became positive for HLA-DR after IFN-γ treatment (Fig. 6P), but the expression level is significantly lower compared with that of the hMSCs. The same results were detected for cells in high passage (data not shown).

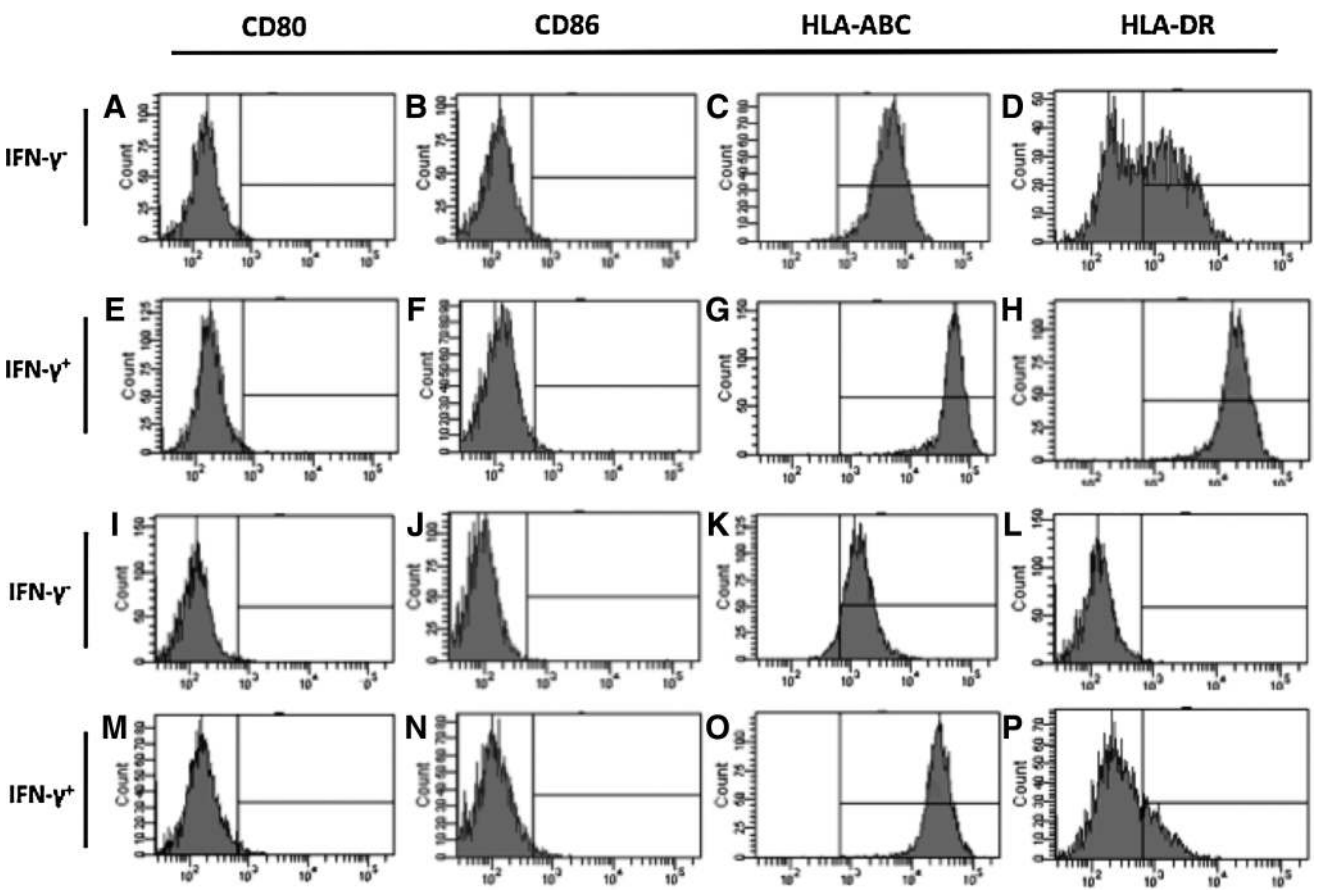

FIG. 6. Flow cytometry analysis of CD80 (**A, E, I, M**), CD86 (**B, F, J, N**), HLA-ABC (**C, G, K, O**), and HLA-DR (**D, H, L, P**) for hMSCs (**A–D**) and hES-MPs (**I–L**). Analyses of the same markers after interferon-γ (IFN-γ) treatment for hMSCs (**E–H**) and hES-MPs (**M–P**).

Discussion

The main questions addressed in this study were how the transcriptome is affected by the process of hES-MP derivation, and how distinct or equivalent cell types the hESCs and the hESC-derived hES-MPs are. Our results from hierarchical cluster analysis, scatter plot analysis, and Spearman correlation analysis all demonstrated that our straightforward protocol for derivation of hES-MPs results in a cell line highly similar to hMSCs, which is in accordance with earlier results from our laboratory.[7] These transcriptional alterations occurring during hES-MP derivation result in a significantly decreased transcription of genes known to be specifically expressed in hESCs. For instance, the *OCT* family of genes (*POU5F1*, *POU5F1P3*, and *POU5F1P4*) as well as *NANOG* are essential transcription factors involved in the maintenance of pluripotency with exclusive expression in ES cells.[18–21] In accordance, *SOX2*, which has been found to form a complex with *OCT4* and bind to the *NANOG* promoter in hESCs,[22] was shown to be highly expressed in hESCs and down-regulated during hES-MP derivation to a level similar that in hMSCs. A similar expression pattern was observed for other genes important for pluripotency, including *TDGF1*, *LIN28*, *GDF3*, *ALPL*, *GAL*, *DPPA4*, *GABRB3*, and *ZIC3*.[15,23–28] Repression of these genes detected during hES-MP derivation thus provides the molecular evidence for the lineage commitment detected in hES-MPs compared with hESCs.[7]

Pluripotency is strongly associated with teratoma formation, and one of the most well-known genes to induce these processes is *TDGF1*.[29,30] The same expression pattern was detected for *EPHA1*, which is overexpressed in many tumors, and *DNMT3B*, which is known to inhibit tumor suppressor genes.[31,32] Another important gene for tumor development is *p53*, whose inactivation is a common feature in many tumors and whose transcription is induced by binding of NR2F2 to the p53 promoter.[33] Significantly increased expression of *NRF2F* during hES-MP formation, as well as altered expression of the *p53*-associated genes *LTBP2* and *TFAP2A*, is thus yet another way for the hES-MP cells to decrease their tumorigenicity.[34,35] Identified hub genes induced by hES-MP derivation include *THBS1*, known to inhibit angiogenesis, as well as the tumor suppressor *CDKN2A* (*p16*) and *CAV1*.[36,37] The tumor-associated gene *EWSR1* was identified as the only hub for genes with a reduced expression pattern during the process of hES-MP derivation. This study thus provides the molecular clues for the lack of teratoma formation detected in the hES-MPs, which is a prerequisite for possible future clinical applications.

With regard to genes associated with proliferation, a panel of such genes (*HELLS*, *CDC25A*, *MCM5*, *FGF5*, *BUB1*, and *ORC1L*) was significantly downregulated during hES-MP derivation, but hES-MPs still had significantly higher expression of these genes compared with hMSCs. *HELLS* is ubiquitously expressed in rapidly dividing cells,[38,39] and targeted disruption of *HELLS* leads to increased replicative senescence along with altered gene expression pattern, particularly the senescence-related genes such as *CDKN2A* and *BMI1*.[40] Moreover, *CDKN2A* is one of the hub genes identified in the process of hES-MP derivation as discussed above. The hES-MPs further displayed significantly higher expression of *MCM10*, *MCM5*, and *ORC1L* required for DNA replication, the mitogen *FGF5*, and *CDC25A* known to accelerate S-phase entry.[41–44] Another pathway inducing proliferation activated during hES-MP derivation was signaling via EGF, and increased expression of *HBEGF*, the receptor *EGFR*, and its ligand *EREG* was detected.[45] Other signaling pathways seem to regulate hMSC proliferation, including the FOS family of transcription factors inducing quiescent cells to reenter the cell cycle.[46] This protein together with *JUN*, which was identified as a hub gene with increased expression in hMSCs, forms the AP-1 complex.[47] The expression pattern of genes in hES-MPs resulting in increased proliferative potential is in line with the high proliferative capacity of these cells (shorter PD time and retained proliferative potential over extended time) compared with hMSCs demonstrated in this study. Decreased proliferative potential of hMSCs during long-term *in vitro* culture has earlier been demonstrated and has to some extent been explained by the decreasing telomere length.[48] The high proliferative potential of the hES-MPs is further in accordance with the presence of longer telomeres compared with the hMSCs, while no differences in telomerase activity was detected. The differences in telomere length observed between hES-MPs and hMSCs may be associated with the intrinsic different source of the two cell types. Isolation from adult donors implies that hMSCs have undergone a higher number of cell divisions, resulting in the shortening of their telomeric sequences. hMSCs displayed increased telomeric length at PD50, suggesting that other mechanisms, known as alternative lengthening of telomeres, which are recognized to be involved in oncogenic transformation,[49] may become activated in hMSCs after protracted expansion. From a different standpoint, these data can be interpreted as results of natural selections, where cells carrying an advantageous ability to keep their telomeric sequences take over the culture and eventually represent the only population of cells able to proliferate for long time. The higher proliferative potential of the hES-MPs provides these cells with a great advantage over hMSCs for bulk production of cells for therapy and tissue engineering applications.

During each cell division cycle, the newly duplicated chromosomes must be distributed evenly into the new cells so that each cell receives exactly one copy of each chromosome. Errors in this process result in aneuploidy that is manifested in genetic disorders and tumors. Accurate sister chromatid segregation relies on the attachment and alignment of chromosomes to the mitotic spindle. This process is controlled by the spindle assembly checkpoint, which restrains cells from entering anaphase until all replicated chromatids have formed proper attachments to a functional bipolar spindle. Several genes encoding proteins constituting this complex, such as *CDC20*, *MAD2*, *BUB1B*, *NDC80*, *NUF2*, *CENPA*, *ERCC6L*, *SPC24*, *MLF1IP*, *AURKB*, *D40*, *SPC25*, *CENPM*, *ZWINT*, and *CDCA8*, were identified as hub genes with significantly increased expression in hES-MPs compared with hMSCs (for review, see Bharadwaj and Yu[50]). Inactivation of certain checkpoint genes results in early embryonic lethality, high levels of chromosome mis-segregation, and apoptosis.[51] The identification of these hub genes overexpressed in hES-MPs demonstrates a strong control function of mitosis important to reduce the risk of tumor formation.

Analyzing expression of 48 genes overexpressed in hESCs compared with differentiated cells demonstrated that hES-MPs derivation results in a more differentiated cellular phenotype consistent with its lineage commitment discussed above and increased expression of markers downregulated in hESCs compared with differentiated cell types. hES-MP derivation did not result in altered expression of genes encoding keratins (*KRT18*, *KRT19*, *KRT7*, and *KRT8*) demonstrating lack of differentiation into the ectodermal lineage. Decreased expression of several claudins (*CLDN3*, *CLDN6*, *CLDN8*, *CLDN10*, and *CYP26A1*) known to be important for retinoic acid metabolism during endodermal differentiation and the early neural marker *CRMP1* demonstrates lack of differentiation into the endodermal lineage during hES-MP derivation.[52,53] The above results are in accordance with the findings previously observed, where hES-MPs were found to be negative for markers typical of the ectodermal and endodermal lineage.[7] In contrast, a panel of genes encoding collagen and other genes characteristic for mesodermal tissues (*COL1A1*, *COL1A2*, *COL3A1*, *COL5A1*, *COL11A1*, *COL6A1*, *COL6A2*, *DDR2*, *BGN*, *FN1*, *FBN1*, and *MFAP5*) and proteins important for cell-to-cell contact or attaching cells to the extracellular matrix (CD44, CD58, CD47, and CD166) were induced by hES-MP derivation to a level similar that in hMSCs.[54]

Other signs of lineage commitment into the mesodermal lineage include increased expression of genes encoding membrane receptors responsive to growth factors inducing mesodermal differentiation (*TGFBR2* and *BMPR2*),[55] and overexpression of *RUNX2*[56] and *TFAP2A*,[57] known to be expressed during osteogenic differentiation. This differentiation into the mesodermal lineage detected might be due to significantly decreased expression of *LEFTY1* detected during hES-MP derivation. Lefty 1 is known to block Nodal signaling by binding Nodal and its coreceptors such as TDGF1. This binding prevents the assembly of an active Nodal/Activin receptor complex, resulting in inhibited mesodermal development.[58,59] The only gene coding for an extracellular matrix component that displayed higher expression in hES cells than in hES-MPs was *LAMA1*. This gene is involved in embryonic patterning and is one of the few essential extracellular matrix proteins in early embryogenesis.[60] It is further significantly downregulated upon development and ES cell differentiation, which is consistent with its decreased expression during hES-MP formation.[61] Induction of these mesodermal markers by hES-MP derivation to the same extent as seen in hMSCs demonstrates the potential of the hES-MP cells in tissue engineering of mesodermal tissues.[62] These data further corroborate previous results demonstrating the *in vitro* and

in vivo differentiation of hES-MPs into tissues of the mesodermal lineage.[7]

The most overexpressed transcription factors detected in hMSCs compared with hES-MPs were *HOXA9*, *HOXA10*, and their downstream effector *IRX3*, whose expression pattern indicates a suppression of erythroid differentiation in hMSCs, reflecting the origin of these cells and the need for this system to maintain the cells undifferentiated.[63] On the other hand, the most highly upregulated transcription factor in hES-MPs compared with hMSCs was *LHX8*, which is essential for tissue patterning and differentiation during embryogenesis.[64] Other transcription factors upregulated in hES-MPs compared with hMSCs were *SALL1*, *PAX3*, *MSX1*, *DLX1*, *DLX2*, and *LZTS1*. *SALL1* is known to play a function in limb cartilage morphogenesis,[65] while *PAX3* promotes myogenic differentiation during vertebrate development.[66] High expression of *DLX1*, *DLX2*, and *MSX1*, supporting craniofacial development and osteogenesis,[67,68] underscores the potential of hES-MPs for mesodermal tissue engineering.

Increased expression of the tumor suppressor gene *LZTS1* in hES-MPs compared with hMSCs may represent an ideal characteristic for clinical applications of these cells.[69–71]

Most of the extracellular matrix components retrieved when comparing hES-MPs and hMSCs displayed a significant upregulation in hMSCs, indicating a more adult phenotype of the hMSCs. In relation to this assumption, the majority of these genes were further downregulated in hESCs compared with hES-MPs, suggesting that hES-MPs may represent an intermediate differentiation state between embryonic and adult stem cells.

The immunological profile of the hES-MPs is highly important for their possible future use in tissue engineering and cell therapy. hES-MPs displayed somewhat lower expression of HLA-ABC compared with hMSCs and significantly lower expression of HLA-DR. Transplantation of an allograft elicits a cascade of host responses *in vivo*, including secretion of IFN-γ, one of the most potent inflammatory cytokines, which further is known to stimulate expression of HLA molecules.[72] The significantly lower induction of HLA-DR in hES-MPs, as opposed to the response in hMSCs, demonstrates that hES-MPs are more immuno-privileged than the hMSCs, and therefore represent a suitable alternative for *in vivo* applications.

Conclusion

As far as we know, this is the first comprehensive study reporting the profound transcriptional changes occurring during hES-MP derivation, resulting in a gene expression profile highly similar to that of hMSCs. These results, in combination with the immunological properties of the hES-MPs reported in this study and the significantly increased proliferative potential of these cells compared with hMSCs, demonstrate that hES-MPs represent a valuable alternative to hMSCs in tissue engineering applications. This data set will also be a valuable resource to the research community to distinguish hES-MPs from hESCs.

Acknowledgment

We sincerely thank Helena Brisby for providing bone marrow samples, and Gunilla Caisander and Annelie Wigander for excellent technical assistance with the immunohistochemical analysis. We acknowledge BIOMATCELL VINN Excellence Center of Biomaterials and Cell Therapy, Region Västra Götland, Swedish Research Council (K2009-52X-09495-22-3 and 2005-7544) and JOIN(ed)T Marie Curie Action for the financial support of the study.

Disclosure Statement

No competing financial interests exist.z

References

1. Tapp, H., Hanley, E.N., Jr., Patt, J.C., and Gruber, H.E. Adipose-derived stem cells: characterization and current application in orthopaedic tissue repair. Exp Biol Med (Maywood) **234,** 1, 2009.
2. Matsumoto, T., Kuroda, R., Mifune, Y., Kawamoto, A., Shoji, T., Miwa, M., Asahara, T., and Kurosaka, M. Circulating endothelial/skeletal progenitor cells for bone regeneration and healing. Bone **43,** 434, 2008.
3. Granero-Molto, F., Weis, J.A., Longobardi, L., and Spagnoli, A. Role of mesenchymal stem cells in regenerative medicine: application to bone and cartilage repair. Expert Opin Biol Ther **8,** 255, 2008.
4. Jukes, J.M., Both, S.K., Leusink, A., Sterk, L.M., van Blitterswijk, C.A., and de Boer, J. Endochondral bone tissue engineering using embryonic stem cells. Proc Natl Acad Sci USA **105,** 6840, 2008.
5. Ringe, J., Kaps, C., Burmester, G.R., and Sittinger, M. Stem cells for regenerative medicine: advances in the engineering of tissues and organs. Naturwissenschaften **89,** 338, 2002.
6. Heins, N., Englund, M.C., Sjöblom, C., Dahl, U., Tonning, A., Bergh, C., Lindahl, A., Hanson, C., and Semb, H. Derivation, characterization, and differentiation of human embryonic stem cells. Stem Cells **22,** 367, 2004.
7. Karlsson, C., Emanuelsson, K., Wessberg, F., Kalic, K., Axell, M.Z., Eriksson, P.S., Lindahl, A., Hyllner, J., and Strehl, R. Human embryonic stem cell-derived mesenchymal progenitors-potential in regenerative medicine. Stem Cell Res **3,** 39, 2009.
8. Xu, C., Jiang, J., Sottile, V., McWhir, J., Lebkowski, J., and Carpenter, M.K. Immortalized fibroblast-like cells derived from human embryonic stem cells support undifferentiated cell growth. Stem Cells **22,** 972, 2004.
9. Barberi, T., Willis, L.M., Socci, N.D., and Studer, L. Derivation of multipotent mesenchymal precursors from human embryonic stem cells. PLoS Med **2,** e161, 2005.
10. Lian, Q., Lye, E., Suan Yeo, K., Khia Way Tan, E., Salto-Tellez, M., Liu, T.M., Palanisamy, N., El Oakley, R.M., Lee, E.H., Lim, B., and Lim S.K. Derivation of clinically compliant MSCs from CD105+, CD24- differentiated human ESCs. Stem Cells **25,** 425, 2007.
11. Olivier, E.N., Rybicki, A.C., and Bouhassira, E.E. Differentiation of human embryonic stem cells into bipotent mesenchymal stem cells. Stem Cells **24,** 1914, 2006.
12. Stojkovic, P., Lako, M., Stewart, R., Przyborski, S., Armstrong, L., Evans, J., Murdoch, A., Strachan, T., and Stojkovic, M. An autogeneic feeder cell system that efficiently supports growth of undifferentiated human embryonic stem cells. Stem Cells **23,** 306, 2005.
13. Karlsson, C., Brantsing, C., Svensson, T., Brisby, H., Asp, J., Tallheden, T., and Lindahl, A. Differentiation of human mesenchymal stem cells and articular chondrocytes:

analysis of chondrogenic potential and expression pattern of differentiation-related transcription factors. J Orthop Res **25,** 152, 2007.
14. Camon, E., Magrane, M., Barrell, D., Lee, V., Dimmer, E., Maslen, J., Binns, D., Harte, N., Lopez, R., and Apweller, R. The gene ontology annotation (GOA) database: sharing knowledge in Uniprot with gene ontology. Nucleic Acids Res **32,** D262, 2004.
15. Assou, S., Le Carrour, T., Tondeur, S., Ström, S., Gabelle, A., Marty, S., Nadal, L., Pantesco, V., Réme, T., Hugnot, J.P., Gasca, S., Hovatta, O., Hamamah, S., Klein, B., and De Vos, J. A meta-analysis of human embryonic stem cells transcriptome integrated into a web-based expression atlas. Stem Cells **25,** 961, 2007.
16. Sturn, A., Quackenbush, J., and Trajanoski, Z. Genesis: cluster analysis of microarray data. Bioinformatics **18,** 207, 2002.
17. Heins, N., Lindahl, A., Karlsson, U., Rehnström, M., Calsander, G., Emanuelsson, K., Hanson, C., Semb, H., Björquist, P., Sartipy, P., and Hyllner, J. Clonal derivation and characterization of human embryonic stem cell lines. J Biotechnol **122,** 511, 2006.
18. Bhattacharya, B., Miura, T., Brandenberger, R., Mejido, J., Luo, Y., Yang, A.X., Joshi, B.H., Ginis, I., Thies, R.S., Amit, M., Lyons, I., Condie, B.G., Itskovitz-Eldor, J., Rao, M.S., and Purl, R.K. Gene expression in human embryonic stem cell lines: unique molecular signature. Blood **103,** 2956, 2004.
19. Pan, G., and Thomson, J.A. Nanog and transcriptional networks in embryonic stem cell pluripotency. Cell Res **17,** 42, 2007.
20. Adewumi, O., Aflatoonian, B., Ahrlund-Richter, L., Amit, M., Andrews, P.W., Beighton, G., Bello, P.A., Benvenisty, N., Berry, L.S., Bevan, S., Blum, B., Brooking, J., Chen, K.G., Choo, A.B., Churchill, G.A., Corbel, M., Damjanov, I., Draper, J.S., Dvorak, P., Emanuelsson, K., Fleck, R.A., Ford, A., Gertow, K., Gertsenstein, M., Gokhale, P.J., Hamilton, R.S., Hampl, A., Healy, L.E., Hovatta, O., Hyllner, J., Imreh, M.P., Itskovitz-Eldor, J., Jackson, J., Johnson, J.L., Jones, M., Kee, K., King, B.L., Knowles, B.B., Lako, M., Lebrin, F., Mallon, B.S., Manning, D., Mayshar, Y., McKay, R.D., Michalska, A.E., Mikkola, M., Milelkovsky, M., Minger, S.L., Moore, H.D., Mummery, C.L., Nagy, A., Nakatsujl, N., O'Brien, C.M., Oh, S.K., Olsson, C., Otonkoski, T., Park, K.Y., Passier, R., Patel, H., Patel, M., Pedersen, R., Pera, M.F., Piekarczyk, M.S., Pera, R.A., Reubinoff, B.E., Robins, A.J., Rossant, J., Rugg-Gunn, P., Schulz, T.C., Semb, H., Sherrer, E.S., Siemen, H., Stacey, G.N., Stojkovic, M., Suemori, H., Szatkiewicz, J., Turetsky, T., Tuuri, T., van den Brink, S., Vintersten, K., Vuoristo, S., Ward, D., Weaver, T.A., Young, L.A., and Zhang, W. Characterization of human embryonic stem cell lines by the International stem cell initiative. Nat Biotechnol **25,** 803, 2007.
21. Hyslop, L., Stojkovic, M., Armstrong, L., Walter, T., Stojkovic, P., Przyborski, S., Herbert, M., Murdoch, A., Strachan, T., and Lako, M. Downregulation of NANOG induces differentiation of human embryonic stem cells to extraembryonic lineages. Stem Cells **23,** 1035, 2005.
22. Rodda, D.J., Chew, J.L., Lim, L.H., Loh, Y.H., Wang, B., Ng, H.H., and Robson, P. Transcriptional regulation of nanog by OCT4 and SOX2. J Biol Chem **280,** 24731, 2005.
23. Lim, L.S., Loh, Y.H., Zhang, W., Li, Y., Chen, X., Wang, Y., Bakre, M., Ng, H.H., and Stanton, L.W. Zic3 is required for maintenance of pluripotency in embryonic stem cells. Mol Biol Cell **18,** 1348, 2007.
24. Yu, J., Vodyanik, M.A., Smuga-Otto, K., Antosiewicz-Bourget, J., Frane, J.L., Tian, S., Nie, J., Jonsdottir, G.A., Ruotti, V., Stewart, R., Slukvin, I.I., and Thomson, J.A. Induced pluripotent stem cell lines derived from human somatic cells. Science **318,** 1917, 2007.
25. Babaie, Y., Herwig, R., Greber, B., Brink, T.C., Wruck, W., Groth, D., Lehrach, H., Burdon, T., and Adjaye, J. Analysis of Oct4-dependent transcriptional networks regulating self-renewal and pluripotency in human embryonic stem cells. Stem Cells **25,** 500, 2007.
26. Boyer, L.A., Lee, T.I., Cole, M.F., Johnstone, S.E., Levine, S.S., Zucker, J.P., Guenther, M.G., Kumar, R.M., Murray, H.L., Jenner, R.G., Gifford, D.K., Melton, D.A., Jaenisch, R., and Young, R.A. Core transcriptional regulatory circuitry in human embryonic stem cells. Cell **122,** 947, 2005.
27. Maldonado-Saldivia, J., van den Bergen, J., Krouskos, M., Gilchrist, M., Lee, C., Li, R., Sinclair, A.H., Surani, M.A., and Western, P.S. Dppa2 and Dppa4 are closely linked SAP motif genes restricted to pluripotent cells and the germ line. Stem Cells **25,** 19, 2007.
28. Inamdar, M.S., Venu, P., Srinivas, M.S., Rao, K., and VijayRaghavan, K. Derivation and characterization of two sibling human embryonic stem cell lines from discarded grade III embryos. Stem Cells Dev **18,** 423, 2009.
29. Ciccodicola, A., Dono, R., Obici, S., Simeone, A., Zollo, M., and Persico, M.G. Molecular characterization of a gene of the EGF family expressed in undifferentiated human NTERA2 teratocarcinoma cells. EMBO J **8,** 1987, 1989.
30. Strizzi, L., Bianco, C., Normanno, N., and Salomon, D. Cripto-1: a multifunctional modulator during embryogenesis and oncogenesis. Oncogene **24,** 5731, 2005.
31. Pasquale, E.B. The Eph family of receptors. Curr Opin Cell Biol **9,** 608, 1997.
32. Rhee, I., Bachman, K.E., Park, B.H., Jair, K.W., Yen, R.W., Schuebel, K.E., Cui, H., Feinberg, A.P., Lengauer, C., Kinzier, K.W., Baylin, S.B., and Vogelstein, B. DNMT1 and DNMT3b cooperate to silence genes in human cancer cells. Nature **416,** 552, 2002.
33. Huang, Q., Raya, A., DeJesus, P., Chao, S.H., Quon, K.C., Caldwell, J.S., Chanda, S.K., Izpisua-Belmonte, J.C., and Schultz, P.G. Identification of p53 regulators by genome-wide functional analysis. Proc Natl Acad Sci USA **101,** 3456, 2004.
34. Yang, H., Filipovic, Z., Brown, D., Breit, S.N., and Vassilev, L.T. Macrophage inhibitory cytokine-1: a novel biomarker for p53 pathway activation. Mol Cancer Ther **2,** 1023, 2003.
35. McPherson, L.A., Loktev, A.V., and Weigel, R.J. Tumor suppressor activity of AP2alpha mediated through a direct interaction with p53. J Biol Chem **277,** 45028, 2002.
36. Li, J., Hassan, G.S., Williams, T.M., Minetti, C., Pestell, R.G., Tanowitz, H.B., Frank, P.G., Sotgia, F., and Lisanti, M.P. Loss of caveolin-1 causes the hyper-proliferation of intestinal crypt stem cells, with increased sensitivity to whole body gamma-radiation. Cell Cycle **4,** 1817, 2005.
37. Rubio, D., Garcia, S., Paz, M.F., De la Cueva, T., Lopez-Fernandez, L.A., Lloyd, A.C., Garcia-Castro, J., and Bernad, A. Molecular characterization of spontaneous mesenchymal stem cell transformation. PLoS ONE **3,** e1398, 2008.
38. Raabe, E.H., Abdurrahman, L., Behbehani, G., and Arceci, R.J. An SNF2 factor involved in mammalian development and cellular proliferation. Dev Dyn **221,** 92, 2001.

39. Geiman, T.M., and Muegge, K. Lsh, an SNF2/helicase family member, is required for proliferation of mature T lymphocytes. Proc Natl Acad Sci USA **97,** 4772, 2000.
40. Sun, L.Q., Lee, D.W., Zhang, Q., Xiao, W., Raabe, E.H., Meeker, A., Miao, D., Huso, D.L., and Arceci, R.J. Growth retardation and premature aging phenotypes in mice with disruption of the SNF2-like gene, PASG. Genes Dev **18,** 1035, 2004.
41. Izumi, M., Yatagai, F., and Hanaoka, F. Cell cycle-dependent proteolysis and phosphorylation of human Mcm10. J Biol Chem **276,** 48526, 2001.
42. Clase, K.L., Mitchell, P.J., Ward, P.J., Dorman, C.M., Johnson, S.E., and Hannon, K. FGF5 stimulates expansion of connective tissue fibroblasts and inhibits skeletal muscle development in the limb. Dev Dyn **219,** 368, 2000.
43. Zhang, X., Neganova, I., Przyborski, S., Yang, C., Cooke, M., Atkinson, S.P., Anyfantis, G., Fenyk, S., Keith, W.N., Hoare, S.F., Hughes, O., Strachan, T., Stojkovic, M., Hinds, P.W., Armstrong, L., and Lako, M. A role for NANOG in G1 to S transition in human embryonic stem cells through direct binding of CDK6 and CDC25A. J Cell Biol **184,** 67, 2009.
44. Ryu, S., Holzschuh, J., Erhardt, S., Ettl, A.K., and Driever, W. Depletion of minichromosome maintenance protein 5 in the zebrafish retina causes cell-cycle defect and apoptosis. Proc Natl Acad Sci USA **102,** 18467, 2005.
45. Komurasaki, T., Toyoda, H., Uchida, D., and Morimoto, S. Epiregulin binds to epidermal growth factor receptor and ErbB-4 and induces tyrosine phosphorylation of epidermal growth factor receptor, ErbB-2, ErbB-3 and ErbB-4. Oncogene **15,** 2841, 1997.
46. Brown, J.R., Nigh, E., Lee, R.J., Ye, H., Thompson, M.A., Saudou, F., Pestell, R.G., and Greenberg, M.E. Fos family members induce cell cycle entry by activating cyclin D1. Mol Cell Biol **18,** 5609, 1998.
47. Fujiki, K., Duerr, E.M., Kikuchi, H., Ng, A., Xavier, R.J., Mizukami, Y., Imamura, T., Kuike, M.H., and Chung, D.C. Hoxc6 is overexpressed in gastrointestinal carcinoids and interacts with JunD to regulate tumor growth. Gastroenterology **135,** 907, 16 e1–2, 2008.
48. Kim, J., Kang, J.W., Park, J.H., Choi, Y., Choi, K.S., Park, K.D., Baek, D.H., Seong, S.K., Min, H.K., and Kim, H.S. Biological characterization of long-term cultured human mesenchymal stem cells. Arch Pharm Res **32,** 117, 2009.
49. Henson, J.D., Neumann, A.A., Yeager, T.R., and Reddel, R.R. Alternative lengthening of telomeres in mammalian cells. Oncogene **21,** 598, 2002.
50. Bharadwaj, R., and Yu, H. The spindle checkpoint, aneuploidy, and cancer. Oncogene **23,** 2016, 2004.
51. Dobles, M., Liberal, V., Scott, M.L., Benezra, R., and Sorger, P.K. Chromosome missegregation and apoptosis in mice lacking the mitotic checkpoint protein Mad2. Cell **101,** 635, 2000.
52. Langton, S., and Gudas, L.J. CYP26A1 knockout embryonic stem cells exhibit reduced differentiation and growth arrest in response to retinoic acid. Dev Biol **315,** 331, 2008.
53. Yocum, A.K., Gratsch, T.E., Leff, N., Strahler, J.R., Hunter, C.L., Walker, A.K., Michallidis, G., Omenn, G.S., O'Shea, K.S., and Andrews, P.C. Coupled global and targeted proteomics of human embryonic stem cells during induced differentiation. Mol Cell Proteomics **7,** 750, 2008.
54. Finnis, M.L., and Gibson, M.A. Microfibril-associated glycoprotein-1 (MAGP-1) binds to the pepsin-resistant domain of the alpha3 (VI) chain of type VI collagen. J Biol Chem **272,** 22817, 1997.
55. Schuldiner, M., Yanuka, O., Itskovitz-Eldor, J., Melton, D.A., and Benvenisty, N. Effects of eight growth factors on the differentiation of cells derived from human embryonic stem cells. Proc Natl Acad Sci USA **97,** 11307, 2000.
56. Komori, T. Runx2, a multifunctional transcription factor in skeletal development. J Cell Biochem **87,** 1, 2002.
57. Fan, Z., Yamaza, T., Lee, J.S., Yu, J., Wang, S., Fan, G., Shi, S., and Wang, C.Y. BCOR regulates mesenchymal stem cell function by epigenetic mechanisms. Nat Cell Biol **11,** 1002, 2009.
58. Sakuma, R., Ohnishi, Yi, Y., Meno, C., Fujii, H., Juan, H., Takeuchi, J., Ogura, T., Li, E., Miyazono, K., and Hamada, H. Inhibition of Nodal signalling by Lefty mediated through interaction with common receptors and efficient diffusion. Genes Cells **7,** 401, 2002.
59. Conlon, F.L., Lyons, K.M., Takaesu, N., Barth, K.S., Kispert, A., Herrmann, B., and Robertson, E.J. A primary requirement for nodal in the formation and maintenance of the primitive streak in the mouse. Development **120,** 1919, 1994.
60. Li, X., Chen, Y., Schéele, S., Arman, E., Haffner-Krausz, R., Ekblom, P., and Lonai, P. Fibroblast growth factor signaling and basement membrane assembly are connected during epithelial morphogenesis of the embryoid body. J Cell Biol **153,** 811, 2001.
61. Hailesellasse Sene, K., Porter, C.J., Palidwor, G., Perez-Iratxeta, C., Muro, E.M., Campbell, P.A., Rudnicki, M.A., and Andrade-Navarro, M.A. Gene function in early mouse embryonic stem cell differentiation. BMC Genomics **8,** 85, 2007.
62. Ivkovic, S., Yoon, B.S., Popoff, S.N., Safadi, F.F., Libuda, D.E., Stephenson, R.C., Daluiski, A., and Lyons, K.M. Connective tissue growth factor coordinates chondrogenesis and angiogenesis during skeletal development. Development **130,** 2779, 2003.
63. Ferrell, C.M., Dorsam, S.T., Ohta, H., Humphries, R.K., Dervnck, M.K., Hagg, C., Largman, C., and Lawrence, H.J. Activation of stem-cell specific genes by HOXA9 and HOXA10 homeodomain proteins in CD34+ human cord blood cells. Stem Cells **23,** 644, 2005.
64. Hobert, O., and Westphal, H. Functions of LIM-homeobox genes. Trends Genet **2,** 75, 2000
65. Kawakami, Y., Uchiyama, Y., Rodriguez Esteban, C., Inenaga, T., Koyano-Nakagawa, N., Kawakami, H., Marti, M., Kmita, M., Monaghan-Nichols, P., Nishinakamura, R., and Izpisua Belmonte, J.C. Sall genes regulate region-specific morphogenesis in the mouse limb by modulating Hox activities. Development **4,** 585, 2009.
66. Gang, E.J., Bosnakovski, D., Simsek, T., To, K., and Perlingeiro, R.C. Pax3 activation promotes the differentiation of mesenchymal stem cells toward the myogenic lineage. Exp Cell Res **8,** 1721, 2008.
67. Merlo, G.R., Zerega, B., Paleari, L., Trombino, S., Mantero, S., and Levi, G. Multiple functions of Dlx genes. Int J Dev Biol **6,** 619, 2000.
68. Satokata, I., Ma, L., Ohehima, H., Bei, M., Woo, I., Nishizawa, K., Maeda, T., Takano, Y., Uchiyama, M., Heaney, S., Peters, H., Tang, Z., Maxson, R., and Maas, R. Msx2 deficiency in mice causes pleiotropic defects in bone growth and ectodermal organ formation. Nat Genet **4,** 391, 2000.
69. Vecchione, A., Croce, C.M., and Baldassarre, G. Fez1/Lzts1 a new mitotic regulator implicated in cancer development. Cell Div **2,** 24, 2007.
70. Califano, D., Pignata, S., Pisano, C., Greggi, S., Laurelli, G., Losito, N.S., Ottaiano, A., Gallipoli, A., Pasquinelli, R.,

De, Simone, V., Cirombella, R., Fusco, A., and Chiappetta, G. FEZ1/LZTS1 protein expression in ovarian cancer. J Cell Physiol **2,** 382, 2010.
71. Vecchione, A., Ishii, H., Baldassarre, G., Bassi, P., Trapasso, F., Alder, H., Pagano, F., Gomella, L.G., Croce, C.M., and Baffa, R. FEZ1/LZTS1 is down-regulated in high-grade bladder cancer, and its restoration suppresses tumorigenicity in transitional cell carcinoma cells. Cancer Epidemiol Biomarkers Prev **2,** 194, 2006.
72. Romieu-Mourez, R., Francois, M., Boivin, M.N., Stagg, J., and Galipeau, J. Regulation of MHC class II expression and antigen processing in murine and human mesenchymal stromal cells by IFN-gamma, TGF-beta, and cell density. J Immunol **179,** 1549, 2007.

Address correspondence to:
Giuseppe Maria de Peppo, M.Sc.
Department of Biomaterials
Sahlgrenska Academy at University of Gothenburg
Box 412, SE 405 30
Göteborg
Sweden

E-mail: giuseppe.de.peppo@biomaterials.gu.se

Received: September 19, 2009
Accepted: February 4, 2010
Online Publication Date: March 10, 2010